



# Analog Circuit Design Laboratory

## Lab Report

**written by:**

Lorenz Buchinger

Agustin Sevil de Llobet

Power Electronics Engineering

FH JOANNEUM – University of Applied Sciences, Austria

**Graz, January 1, 1991**

# Contents

<b>1 Computer Lab .....</b>	<b>1</b>
1.1 Noise Analysis with PSpice .....	1
1.1.1 Task Description .....	1
1.1.2 Schematic .....	1
1.1.3 Curves & Diagrams .....	3
1.1.4 Discussion of Measurement Results .....	4
<b>2 Electronic Lab .....</b>	<b>6</b>
2.1 Active Band-pass Filter .....	6
2.1.1 Task Description .....	6
2.1.2 Schematic .....	6
2.1.3 Formulas and Calculations .....	7
2.1.4 Table(s) with Measurement Results .....	7
2.1.5 Curves & Diagrams .....	9
2.1.6 Discussion of Measurement Results .....	14
2.2 ADC-Driver And Anti-aliasing Filter .....	15
2.2.1 Task Description .....	15
2.2.2 Schematic .....	16
2.2.3 Formulas and Calculations .....	16
2.2.4 Table(s) with Measurement Results .....	20
2.2.5 Curves & Diagrams .....	21
2.2.6 Discussion of Measurement Results .....	24
2.3 Switched Capacitor Filter .....	25
2.3.1 Task Description .....	25
2.3.2 Schematic .....	25

2.3.3	Formulas and Calculations . . . . .	26
2.3.4	Table(s) with Measurement Results . . . . .	29
2.3.5	Curves & Diagrams . . . . .	31
2.3.6	Discussion of Measurement Results . . . . .	34
<b>E</b>	<b>Equipment Used .....</b>	<b>37</b>
<b>A</b>	<b>Appendix .....</b>	<b>38</b>
A.1	Calculations . . . . .	39
	A.1.1 Active Band-pass Filter . . . . .	39
A.2	Matlab . . . . .	42
A.3	Measurements . . . . .	42



1

# Computer Lab

## 1.1 Noise Analysis with PSpice

### 1.1.1 Task Description

The task of this lab session was to conduct simulations of transistor and OpAmp circuits in PSpice, and to analyze the noise generated by the different components of the circuits. The circuits that were simulated include a single stage emitter circuit, an inverting amplifier, and a non-inverting amplifier. The noise spectral voltage density of the output of each circuit was analyzed, and the contribution of each individual resistor to the overall noise was also examined.

### 1.1.2 Schematic

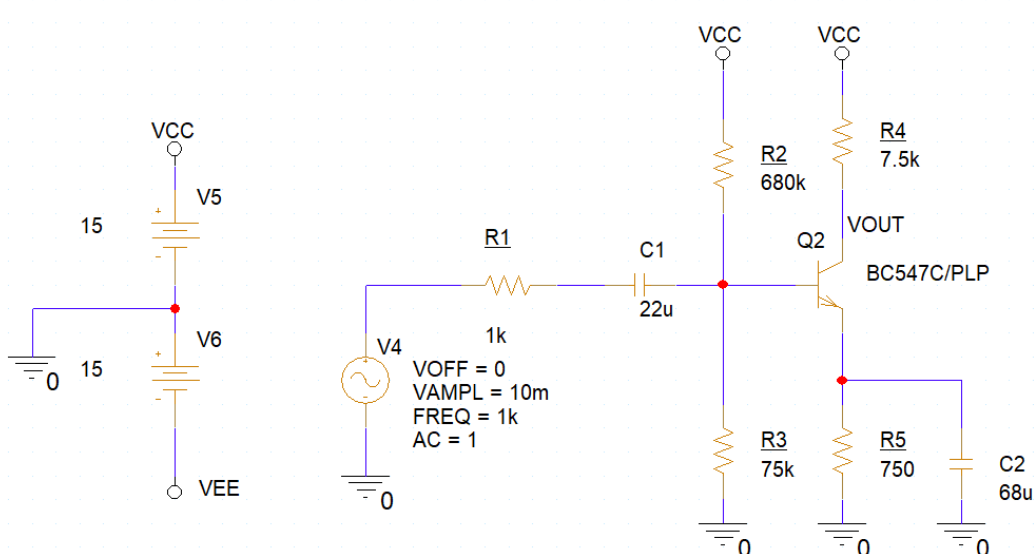


Figure 1.1: Schematic of the single stage emitter circuit used for simulation.

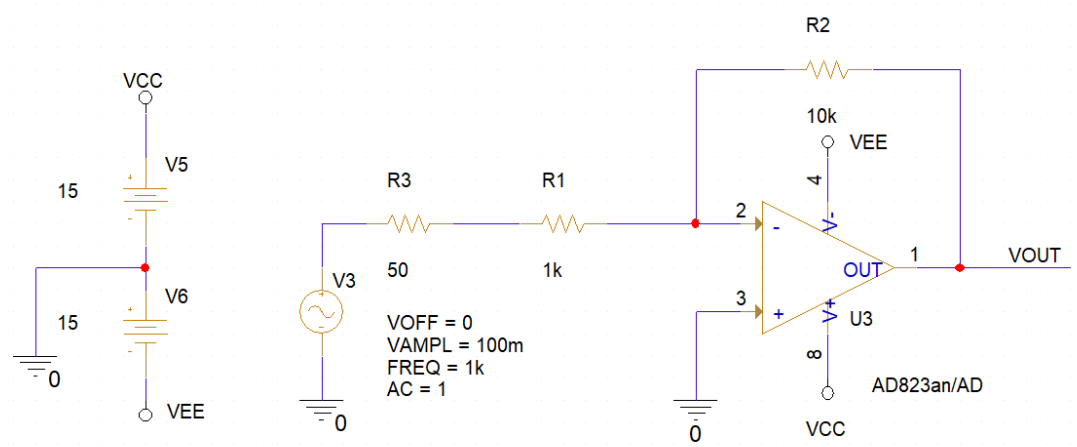


Figure 1.2: Schematic of the inverting amplifier circuit used for simulation.

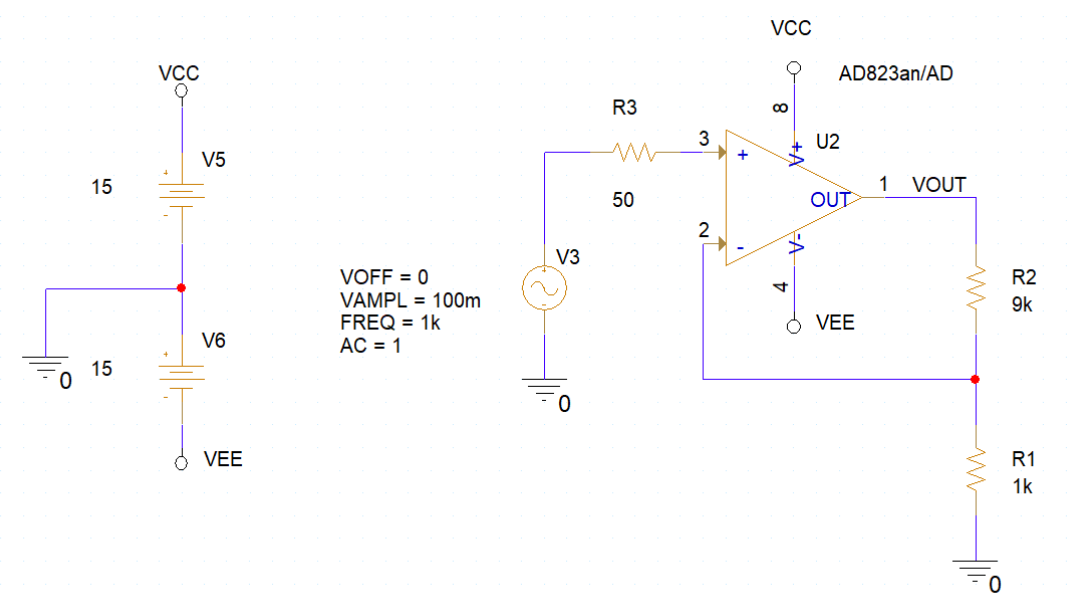


Figure 1.3: Schematic of the non-inverting amplifier circuit used for simulation.

### 1.1.3 Curves & Diagrams

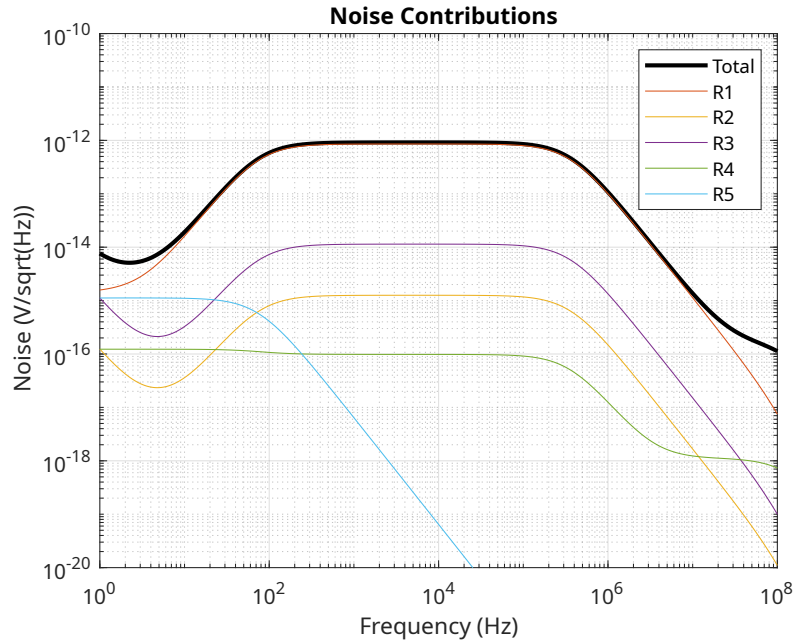


Figure 1.4: Noise spectral voltage density of the single stage emitter circuits output. The simulation results of the noise generated by each individual resistor is also depicted.

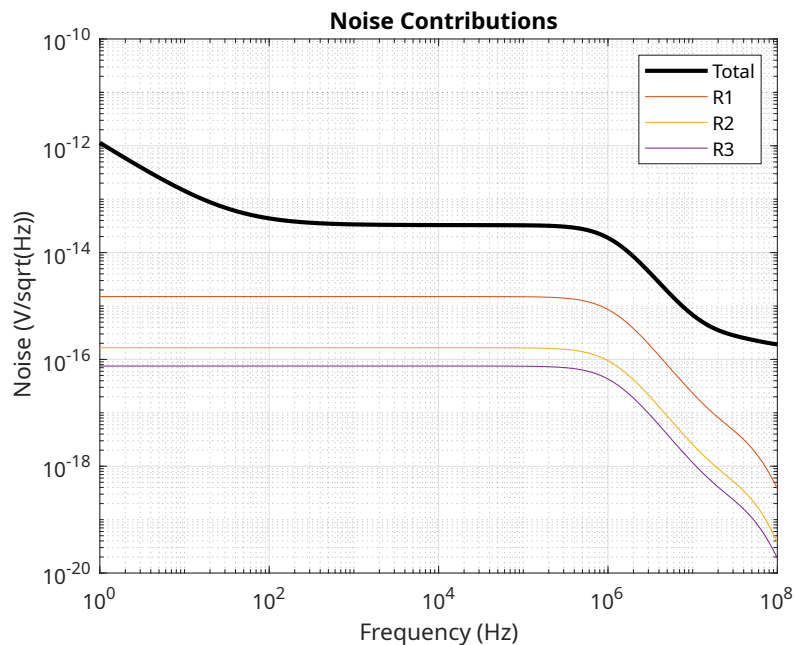


Figure 1.5: Noise spectral voltage density of the inverting amplifiers output. The simulation results of the noise generated by each individual resistor is also depicted.

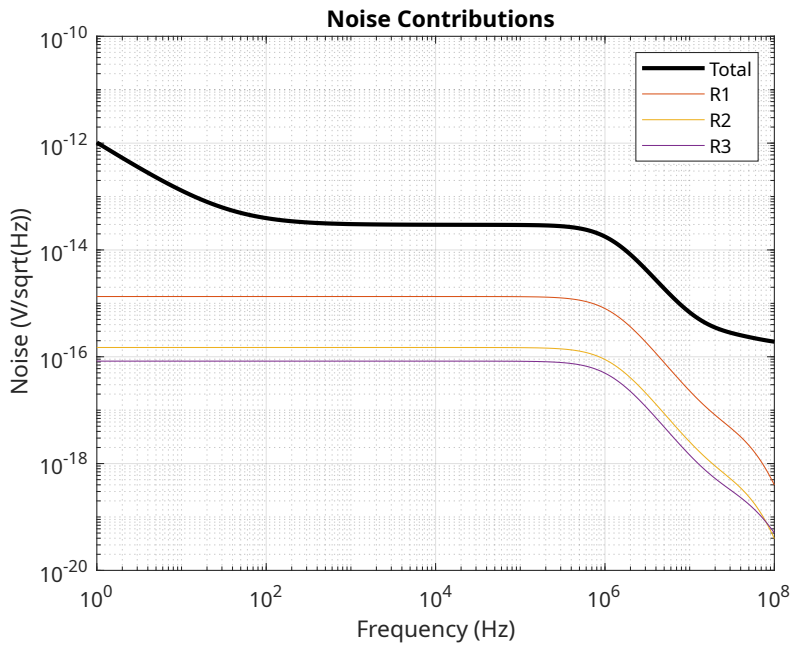


Figure 1.6: Noise spectral voltage density of the non-inverting amplifiers output. The simulation results of the noise generated by each individual resistor is also depicted.

#### 1.1.4 Discussion of Measurement Results

The measured noise spectral voltage density of the emitter follower stage (figure 1.4) shows a similar trend as the emitter followers magnitude response. The emitter follower effectively acts as a bandpass-filter with a very wide pass band. The lower corner frequency of the pass band is determined by the value of the input coupling capacitor and the upper corner frequency by the transistors parasitic capacitances. The thermal noise originating from the resistors is amplified according to the passband characteristics of the emitter follower. R4 and R5 are exceptions because they are not affected by the input coupling capacitor and therefore have no lower corner frequency. R1 is the biggest contributor to the thermal noise even though it has a relatively low resistance because its noise acts as an input signal to the amplifier and is therefore amplified by the gain of the emitter follower.

The shot noise, caused by the transistor, is also visible at lower frequencies. It can be seen when looking at the noise of R3, R4 and the total output noise.

The inverting and non-inverting amplifier stages show an almost identical noise spectral voltage density (figures 1.5 and 1.6). The same behavior observed in the emitter follower where the noise spectral density behaves similar to the magnitude response of the amplifier can also be seen in these two OpAmp amplifier stages. The low-pass filter behavior of the amplifiers can be observed in the

noise spectrum. The OpAmps shot noise is also visible at lower frequencies and can only be evident in the total noise and is not present in the individual resistors noise curves because the shot noise is generated by the OpAmp itself and not by the resistors.

# 2

## Electronic Lab

### 2.1 Active Band-pass Filter

#### 2.1.1 Task Description

A second-order active bandpass filter was designed using the LM4562 dual operational amplifier by cascading two staggered tuned first-order bandpass stages in multi-feedback topology. The transfer function and component values were calculated manually according to the given specifications (Butterworth and 1 dB Chebyshev, 4–5 kHz, 20 dB gain). E24-series components with 1% tolerance were chosen.

The circuit was simulated in PSpice (transient, AC, noise and Monte Carlo analysis), implemented on a prototype board with  $\pm 5$  V supply, and experimentally characterized. Frequency response, passband gain, 3 dB corner frequencies and step response were measured and compared with simulation results in a combined Bode plot.

Finally, the output noise behavior was analyzed and discussed in the report.

#### 2.1.2 Schematic

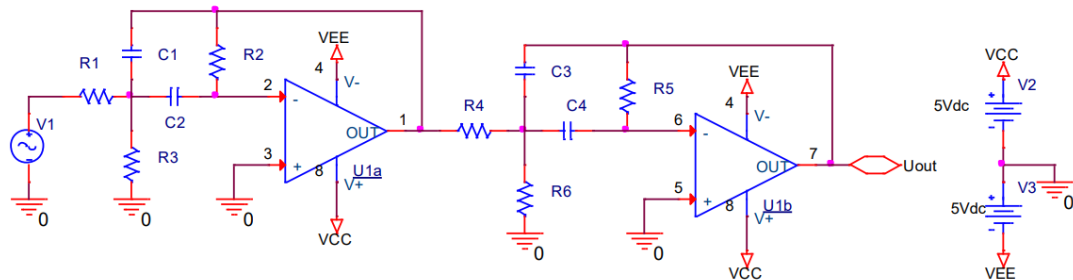


Figure 2.1: Schematic of the second order band pass filter.

### 2.1.3 Formulas and Calculations

The calculations were done by hand. A scan of the hand written notes can be found in section A.1.1 of the appendix

### 2.1.4 Table(s) with Measurement Results

Table 2.1: Component values for Butterworth band-pass filter

	Calculated	Chosen	Measured
$R_1$ in kΩ	5.448	5.6	5.5831
$R_2$ in kΩ	48.880	47	46.943
$R_3$ in Ω	303.59	300	298.59
$R_4$ in kΩ	4.650	4.7	4.6045
$R_5$ in kΩ	41.718	43	42.798
$R_6$ in Ω	259.11	270	269.01
$C_1$ in nF	-	10	10.03
$C_2$ in nF	-	10	10.09
$C_3$ in nF	-	10	10.03
$C_4$ in nF	-	10	10.10

Table 2.2: Component values for Chebyshev 1 dB band-pass filter

	Calculated	Chosen	Measured
$R_1$ in $k\Omega$	7.532	7.5	-
$R_2$ in $k\Omega$	124.641	120	-
$R_3$ in $\Omega$	117.89	120	-
$R_4$ in $k\Omega$	6.492	6.2	-
$R_5$ in $k\Omega$	107.432	110	-
$R_6$ in $\Omega$	101.613	100	-
$C_1$ in $nF$	-	10	10.03
$C_2$ in $nF$	-	10	10.09
$C_3$ in $nF$	-	10	10.03
$C_4$ in $nF$	-	10	10.10

The measured resistor values show deviations below 1% with respect to the nominal chosen E24 values, which confirms the specified tolerance class. The capacitor measurements also confirm the 1% NP0 specification and therefore only introduce minor shifts in the center frequency.

Table 2.3: Center and corner frequencies with their corresponding gain values.

	-3dB Corner Frequency	Center Frequency	+3dB Corner Frequency
Frequency in Hz	4.32	4.57	4.94
Gain in dB	19.3	22.3	19.3

The measurements for the bode plot can be found at the appendix in table A.1.

### 2.1.5 Curves & Diagrams

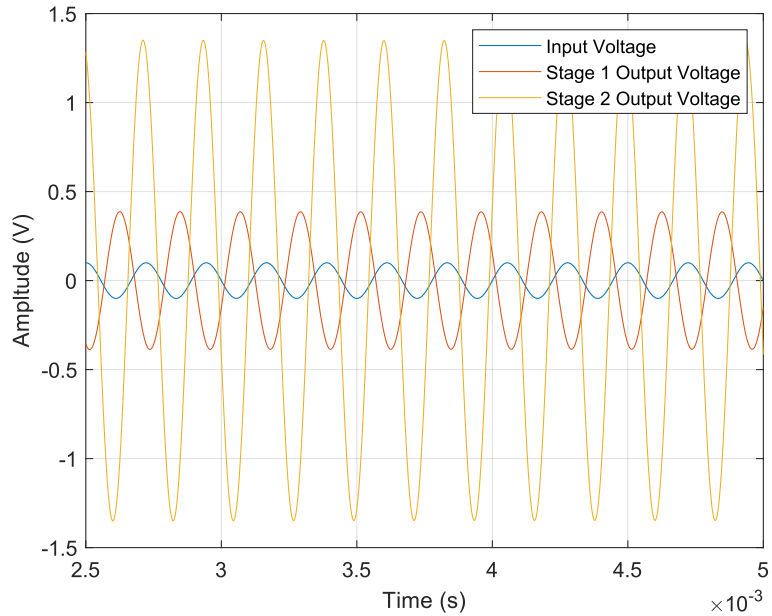


Figure 2.2: Transient simulation showing the sinusoidal input voltage and the output voltage of each of the two amplifier stages.

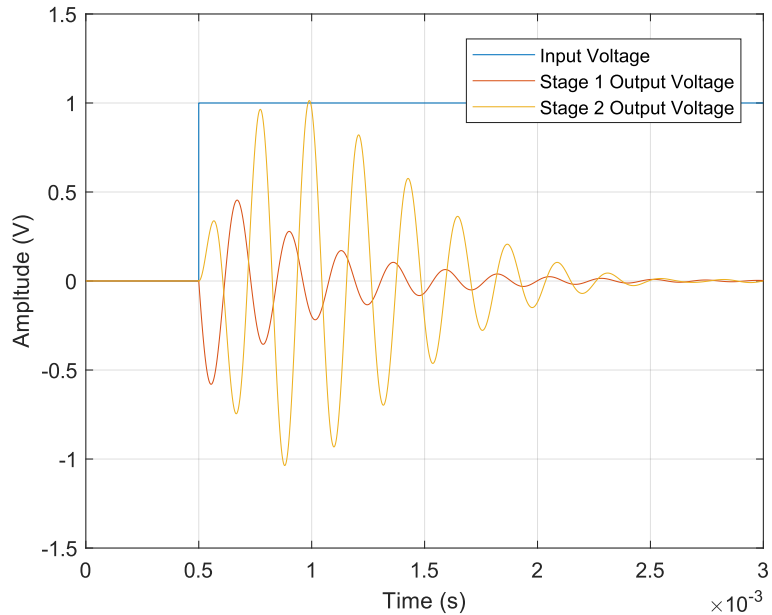


Figure 2.3: Transient simulation showing the step response of both amplifier stages after applying a signal transitioning from 0 V to 1 V to the input.

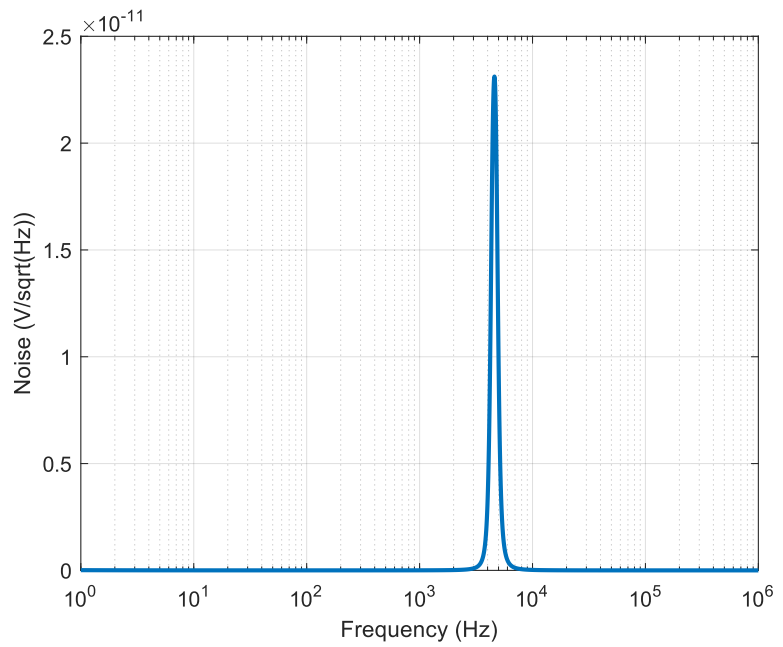


Figure 2.4: Simulation results of the noise spectral voltage density.

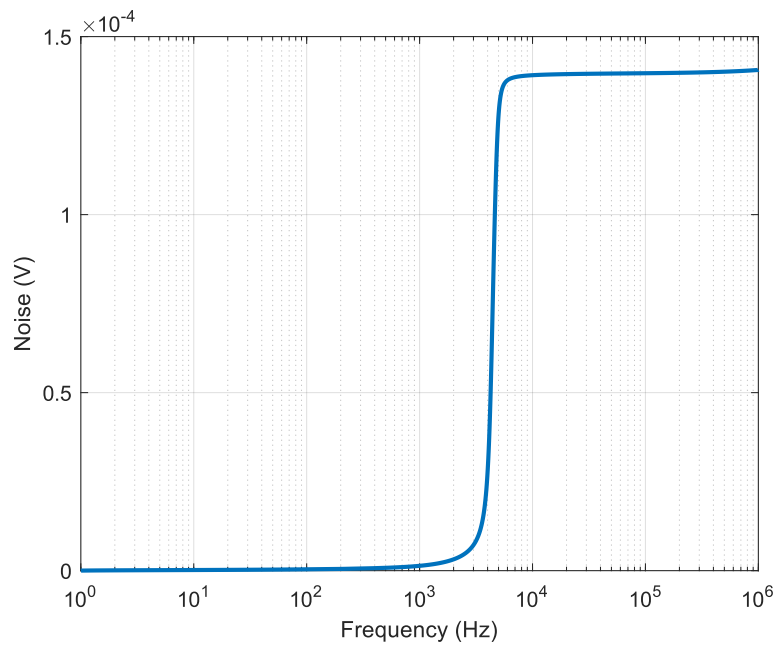


Figure 2.5: Simulation results of the total output noise voltage.

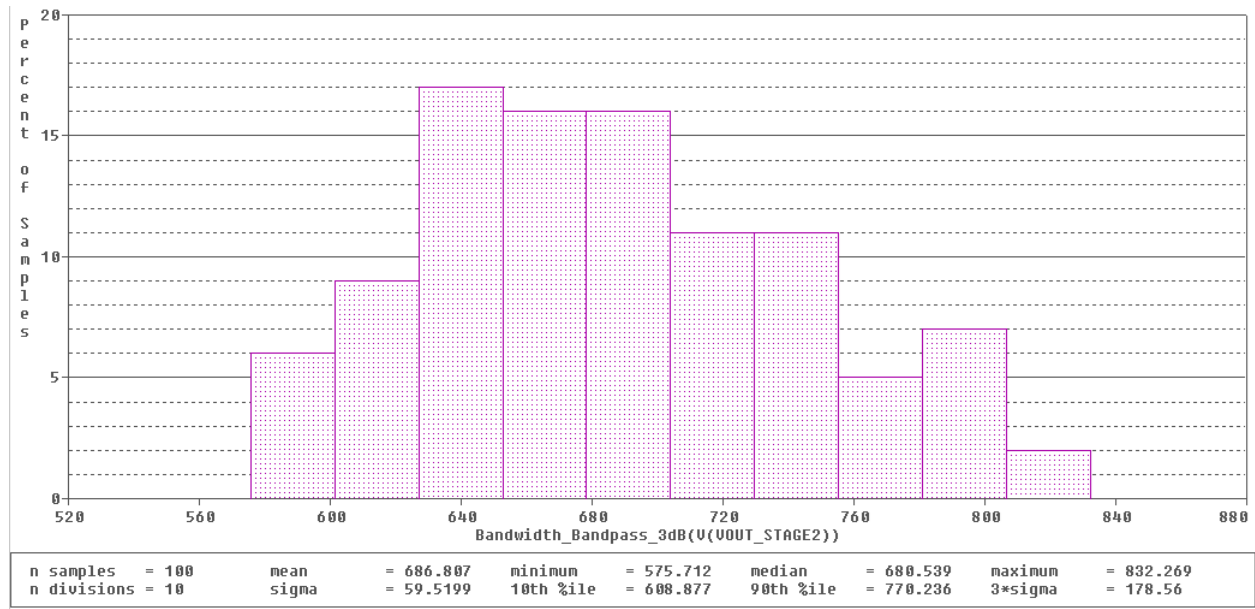


Figure 2.6: Monte Carlo simulation of the 3 db bandwidth. 1% tolerances were used for both resistors and capacitors.

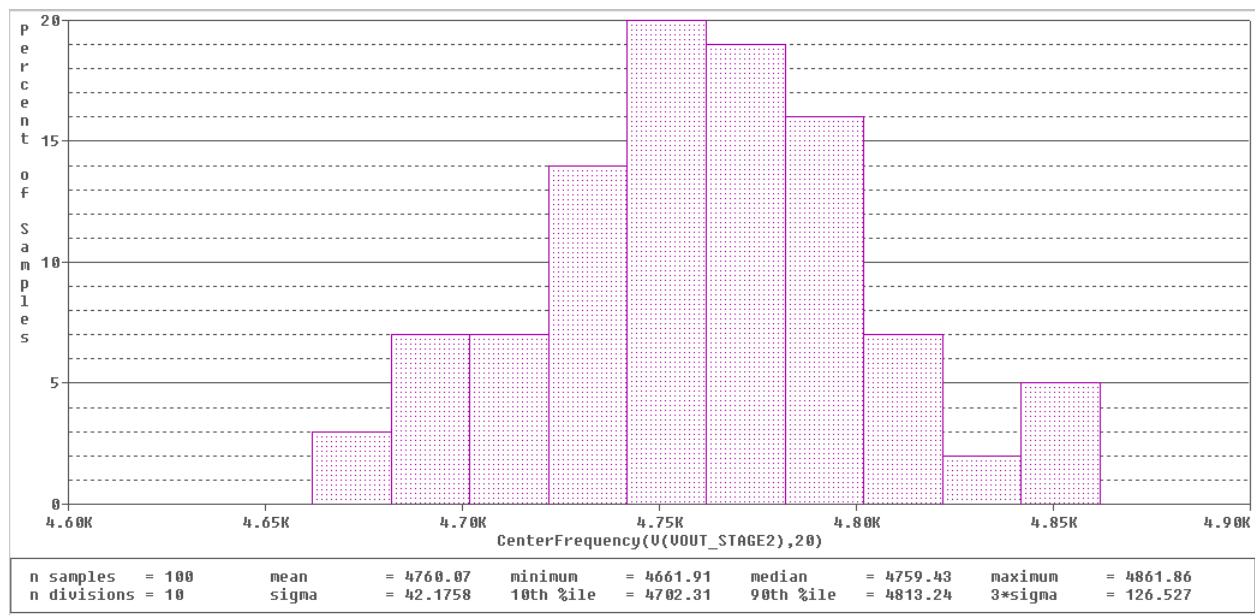


Figure 2.7: Monte Carlo simulation of the center frequency. 1% tolerances were used for both resistors and capacitors.

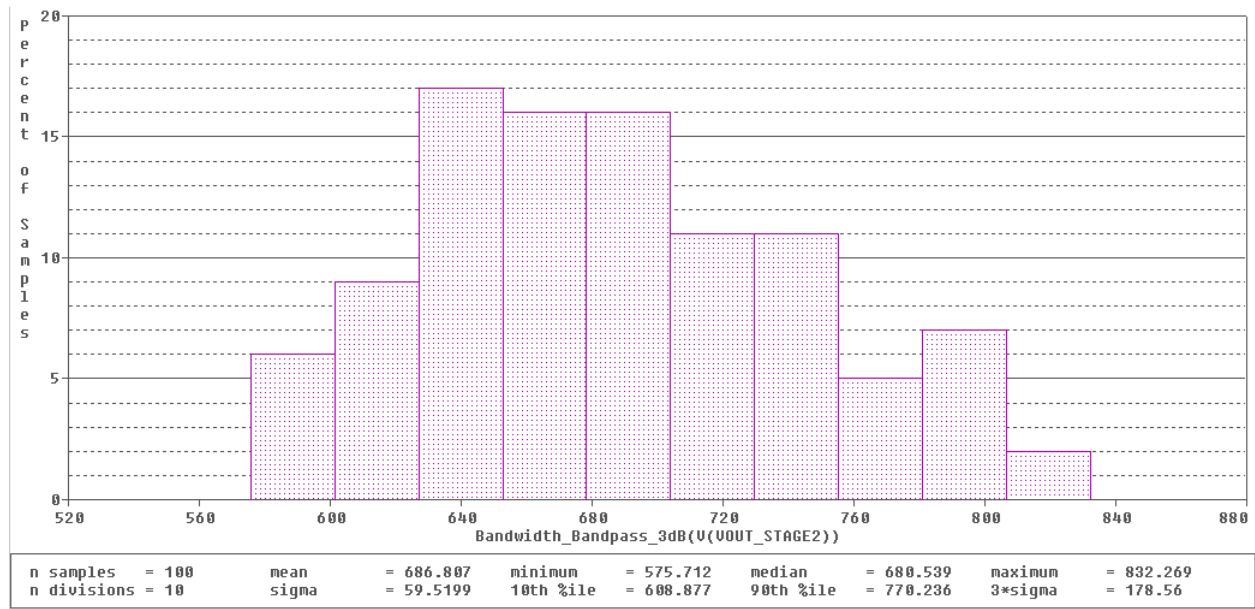


Figure 2.8: Monte Carlo simulation of the gain variation. 1% tolerances were used for both resistors and capacitors.

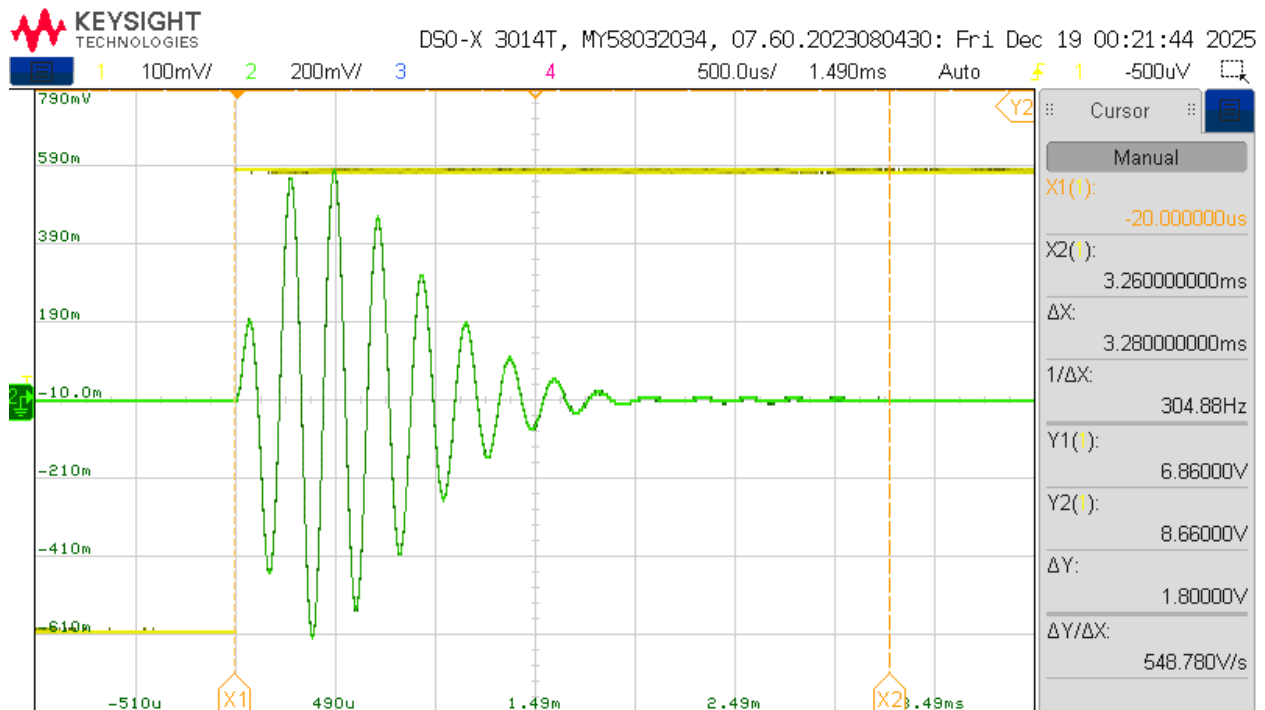


Figure 2.9: Measurement of the filters step response. A 0,5 V square wave was used as the step function.

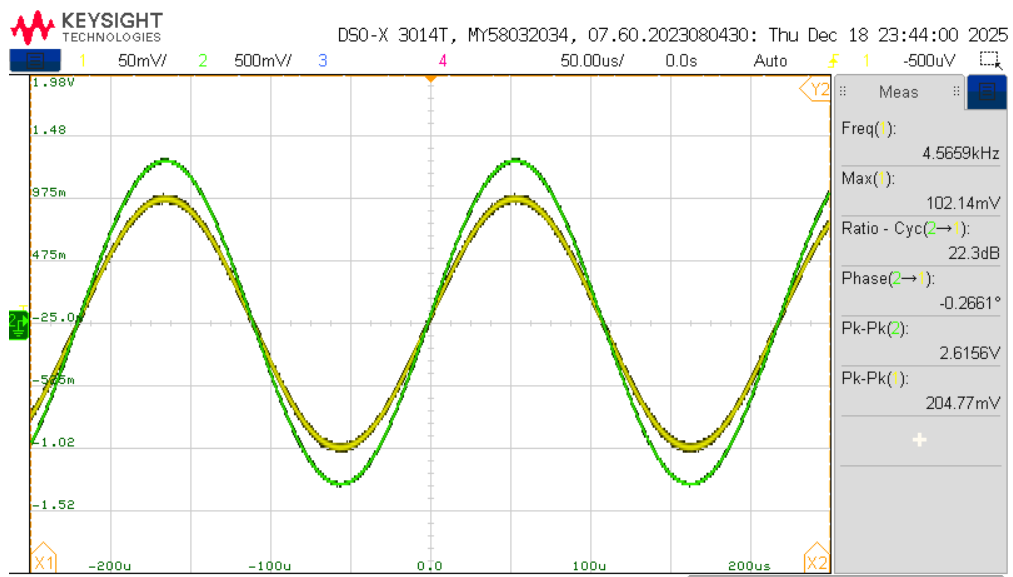


Figure 2.10: Measurement of the passband gain.

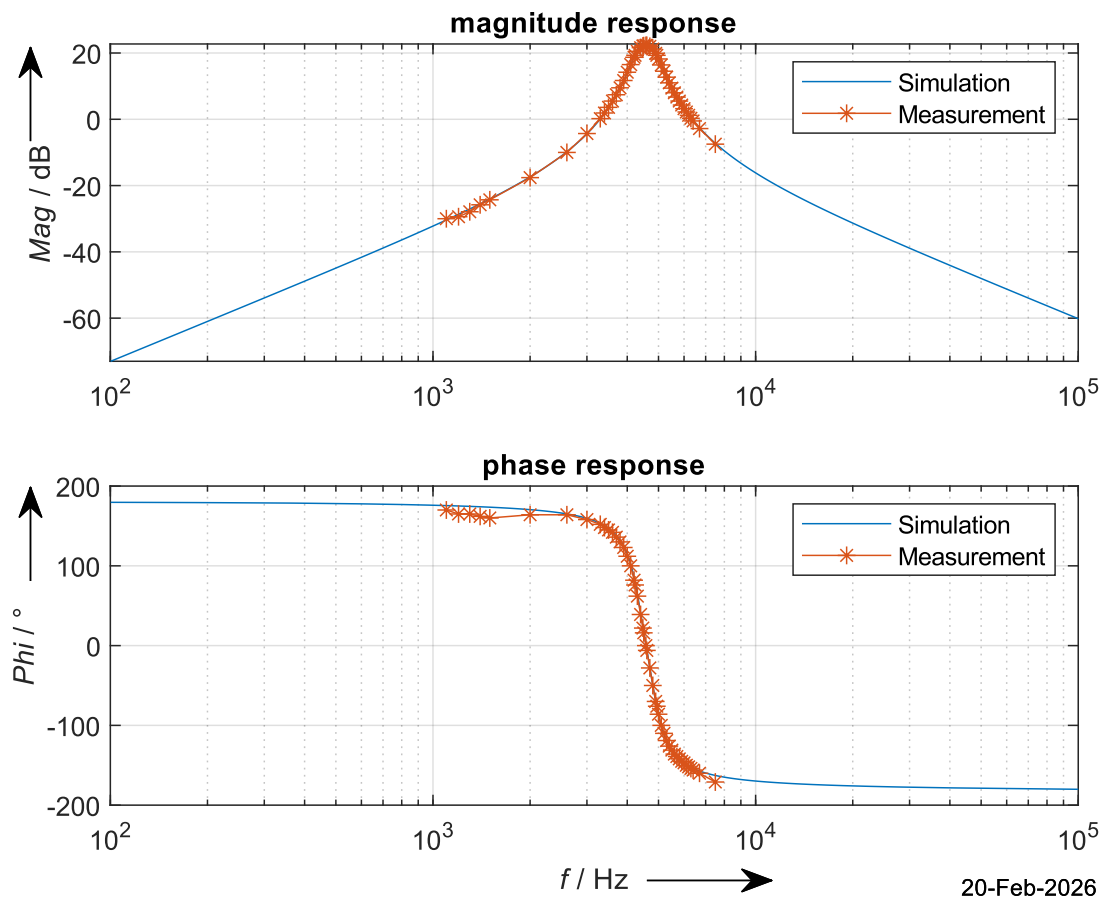


Figure 2.11: Bode plot displaying both simulated and measured values.

### 2.1.6 Discussion of Measurement Results

## 2.2 ADC-Driver And Anti-aliasing Filter

### 2.2.1 Task Description

A single-ended to differential driver for the AD7626 ADC was designed using the LM4562 dual operational amplifier. The circuit includes a second-order active low-pass filter (100 Hz – 40 kHz) with a total differential gain of 20 and a DC offset of 1 V at both outputs.

The circuit was simulated in PSpice (Bode plot, time-domain response and output noise), implemented on a prototype board, and experimentally characterized. Magnitude and phase response, step response, and differential output signals were measured and compared with the simulation results.

Finally, the SNR and ENOB were calculated for a full-scale ADC input signal.

$C_1$	150 pF
$C_2$	4,7 nF
$f_{cl}$	100 Hz
$f_{cu}$	40 kHz
$A_0$	20

Table 2.4: Given values.

## 2.2.2 Schematic

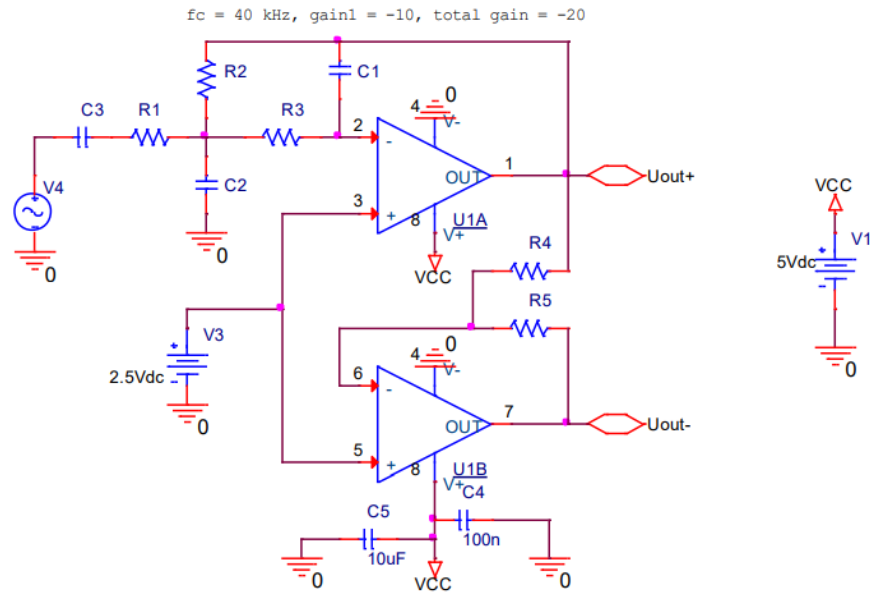


Figure 2.12: Schematic of the ADC driver with anti-aliasing filter

## 2.2.3 Formulas and Calculations

To calculate the component values the general transfer function for

$$H(s) = \frac{H_0}{1 + a \cdot s + b \cdot s^2} \quad (2.1)$$

$$H(P) = -\frac{\frac{R_2}{R_1}}{1 + \omega_c C_1 \left( R_2 + R_3 + \frac{R_2 R_3}{R_1} \right) P + \omega_c^2 C_1 C_2 R_2 R_3 P^2} \quad (2.2)$$

$$H_0 = -\frac{R_2}{R_1} \quad (2.3)$$

$$a = \omega_c C_1 \left( R_2 + R_3 + \frac{R_2 R_3}{R_1} \right) \quad (2.4)$$

$$b = \omega_c^2 C_1 C_2 R_2 R_3 \quad (2.5)$$

$$P = \frac{s}{\omega_c} \quad (2.6)$$

The decision was made to use a Butterworth characteristic for the second order multi-feedback filter. The values for a and b for a Butterworth filter are as follows:

$$a = \sqrt{2} \quad (2.7)$$

$$b = 1 \quad (2.8)$$

$\omega_c$  is calculated according to equation 2.9.

$$\omega_c = 2\pi f_{cu} = 2\pi \cdot 40 \text{ kHz} = 251 \cdot 10^3 \text{ s}^{-1} \quad (2.9)$$

## SNR and ENOB Calculation of the ADC Driver System

The system consists of a single-ended to differential driver implemented with the LM4562 operational amplifier, followed by the AD7626 16-bit ADC. The total system performance is limited by both the ADC quantization noise and the analog front-end noise.

### Ideal ADC SNR

For an ideal N-bit ADC with a full-scale sinusoidal input, the theoretical Signal-to-Noise Ratio (SNR) is given by:

$$SNR_{ideal} = 6.02N + 1.76 \text{ [dB]} \quad (2.10)$$

For a 16-bit ADC:

$$SNR_{ideal} = 6.02 \cdot 16 + 1.76 = 98.08 \text{ dB} \quad (2.11)$$

This value represents the quantization noise limit only.

### Real ADC SNR (Datasheet Value)

According to the AD7626 datasheet, the typical SNR for a full-scale sine wave is:

$$SNR_{ADC} \approx 91.5 \text{ dB} \quad (2.12)$$

This value includes internal non-idealities and thermal noise.

### Analog Driver Signal Level

The input signal to the driver is:

$$V_{in,pp} = 100 \text{ mV} \quad (2.13)$$

The differential gain of the driver is:

$$A_{diff} = 20 \quad (2.14)$$

Therefore, the peak-to-peak voltage at the ADC input is:

$$V_{out,pp} = A_{diff} \cdot V_{in,pp} = 20 \cdot 0.1 = 2 \text{ V} \quad (2.15)$$

### RMS Signal Value at the ADC Input

For a sinusoidal signal:

$$V_{signal,RMS} = \frac{V_{pp}}{2\sqrt{2}} = \frac{2}{2\sqrt{2}} = \frac{2}{2.828} = 0.707 \text{ V} \quad (2.16)$$

### RMS Noise Voltage of the Driver

From PSpice noise simulation over the bandwidth (100 Hz – 40 kHz):

$$V_{noise,RMS} = 40.7 \mu\text{V} \quad (2.17)$$

### Driver SNR

$$SNR_{driver} = \frac{V_{signal,RMS}}{V_{noise,RMS}} = \frac{0.707}{40.7 \times 10^{-6}} = 17375 \quad (2.18)$$

In decibels:

$$SNR_{driver,dB} = 20 \log_{10}(17375) = 84.8 dB \quad (2.19)$$

### Total System SNR

Since ADC noise and driver noise are uncorrelated, they must be combined in linear scale:

$$\frac{1}{SNR_{total}} = \frac{1}{SNR_{ADC}} + \frac{1}{SNR_{driver}} \quad (2.20)$$

First, convert both SNR values to linear scale:

$$SNR_{ADC,lin} = 10^{91.5/10} = 1.41 \times 10^9 \quad (2.21)$$

$$SNR_{driver,lin} = 10^{84.8/10} = 3.02 \times 10^8 \quad (2.22)$$

Combine both contributions:

$$\frac{1}{SNR_{total,lin}} = \frac{1}{1.41 \times 10^9} + \frac{1}{3.02 \times 10^8} \quad (2.23)$$

$$SNR_{total,lin} \approx 2.48 \times 10^8 \quad (2.24)$$

Convert back to decibels:

$$SNR_{total,dB} = 10 \log_{10}(2.48 \times 10^8) = 83.95 dB \quad (2.25)$$

### Effective Number of Bits (System)

$$ENOB = \frac{SNR_{total,dB} - 1.76}{6.02} = \frac{83.95 - 1.76}{6.02} = \frac{82.19}{6.02} = 13.65 bits \quad (2.26)$$

### 2.2.4 Table(s) with Measurement Results

Table 2.5: Component values for ADC driver and anti-aliasing filter

	Calculated	Chosen	Measured
$R_1$ in $\Omega$	-	820	817
$R_2$ in $k\Omega$	-	8.2	8.1602
$R_3$ in $k\Omega$	-	2.7	2.6888
$R_4$ in $k\Omega$	10	10	9.8642
$R_5$ in $k\Omega$	10	10	9.8666
$C_1$ in $pF$	-	150	155
$C_2$ in $nF$	-	4.7	4.61
$C_3$ in $\mu F$	-	1.5	1.56
$C_4$ in $nF$	-	100	-
$C_5$ in $\mu F$	-	10	-

The measured resistor deviations are within the expected 1% tolerance range. The small deviations of the RC components slightly influence the cutoff frequency of the anti-aliasing filter, but remain within acceptable limits. The measured capacitance variation of C1 (150 pF → 155 pF) leads to a minor shift of the pole frequency.

The measurements for the bode plot can be found at the appendix in table A.2

The measured response shows a constant gain of approximately 26 dB within the passband. The phase shift approaches  $-180$  deg at high frequencies, which confirms the expected second-order low-pass behavior. The cutoff frequency can be determined from the  $-3$  dB drop relative to the mid-band gain.

### 2.2.5 Curves & Diagrams

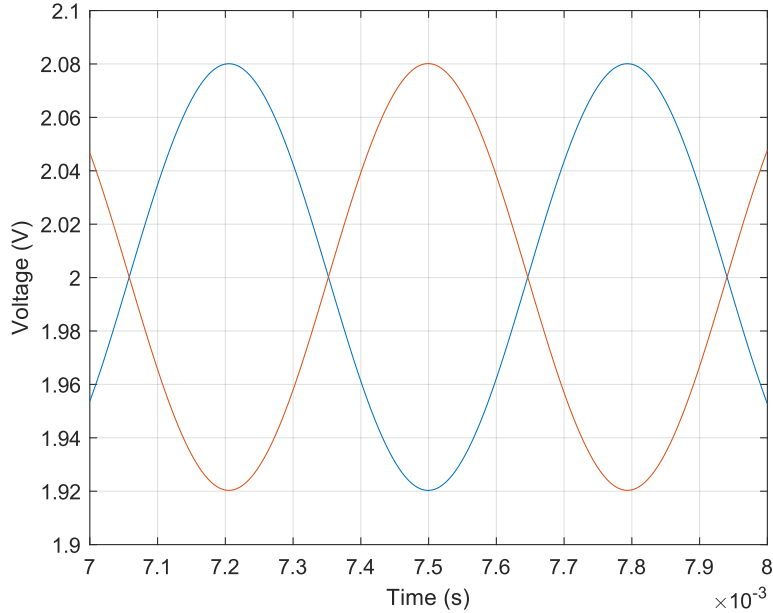


Figure 2.13: Simulation results of the ADC driver and anti-aliasing filter. The blue line shows the non-inverted output, while the orange line shows the inverted output. The offset voltage is 2 V. The input sine wave has an amplitude of 8 mV.

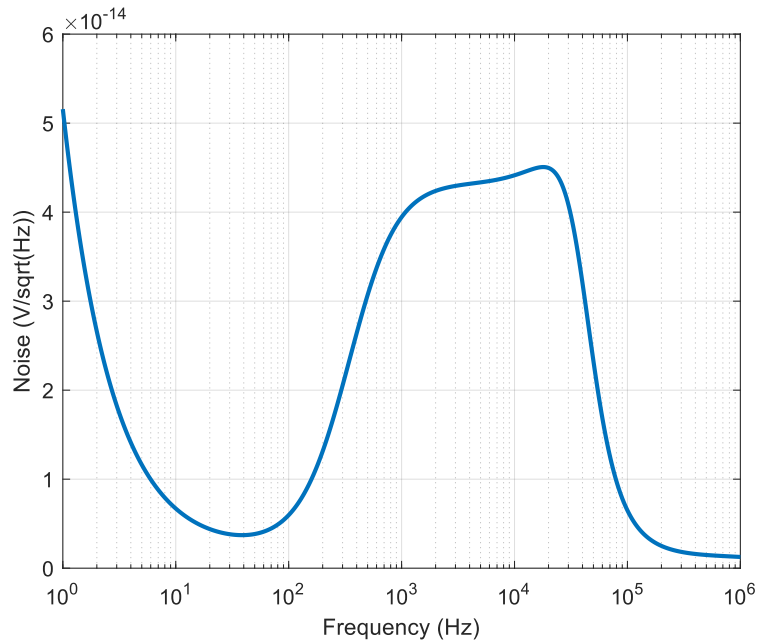


Figure 2.14: Simulation results of the noise spectral voltage density.

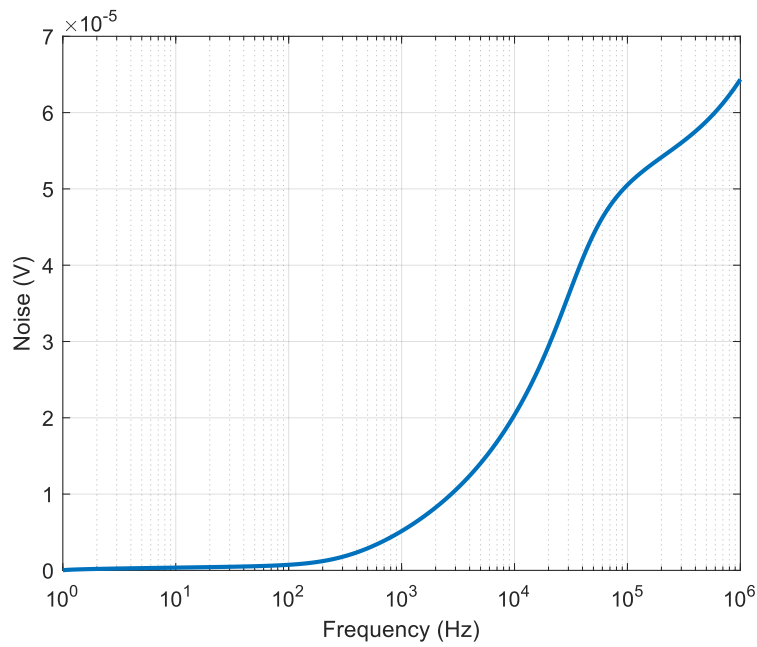


Figure 2.15: Simulation results of the total output noise.

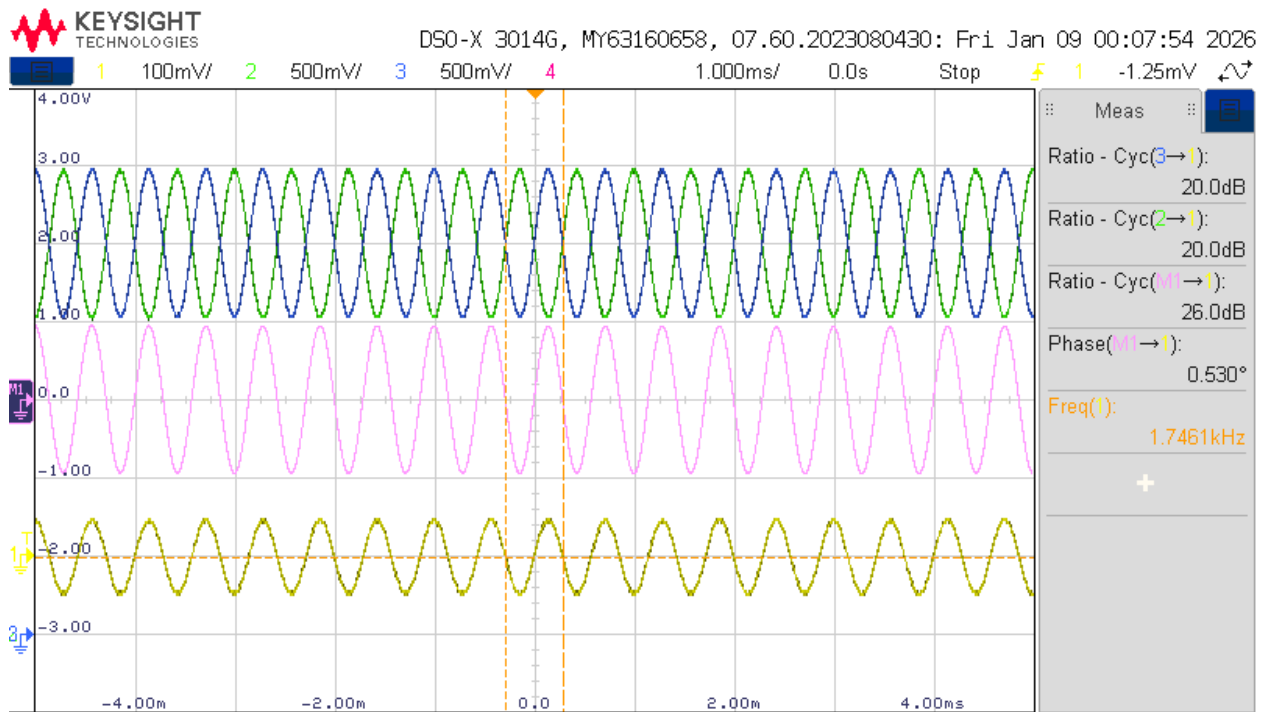


Figure 2.16: Measurements of input signal (yellow), the non-inverting (blue) and inverting (green) output and the differential output (magenta).

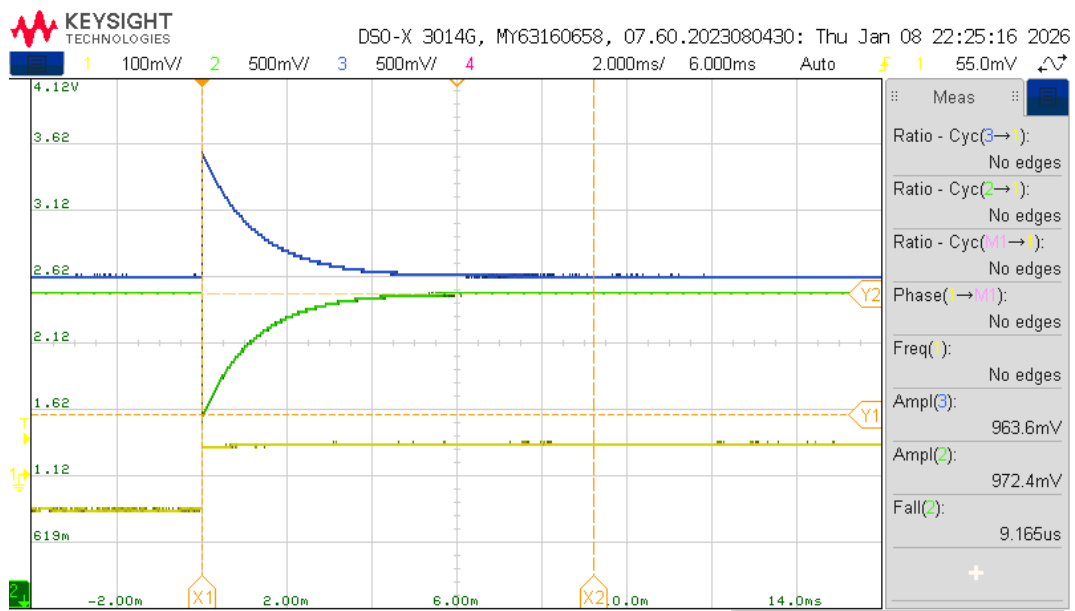


Figure 2.17: Step response of the ADC driver and anti-aliasing filter.

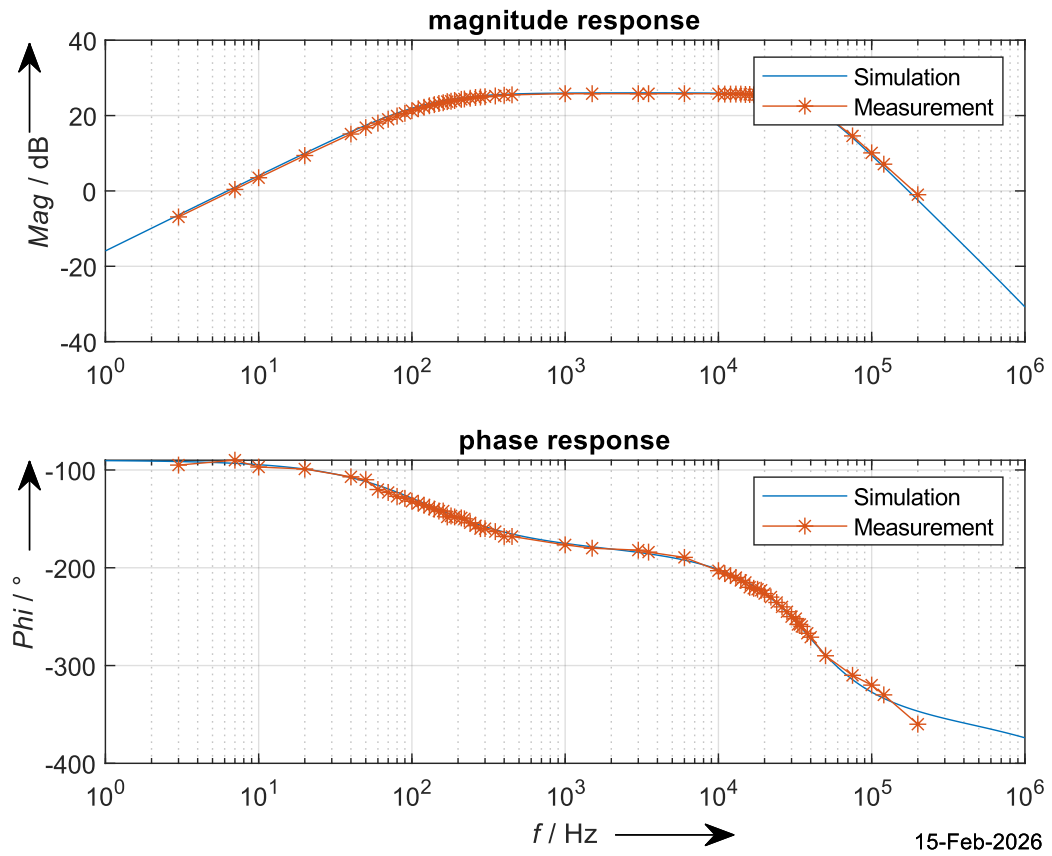


Figure 2.18: Bode plot displaying both simulated and measured values of the differential output.

### 2.2.6 Discussion of Measurement Results

As we can observe in Figure 2.16, the driver correctly amplifies the input signal, providing a differential gain of approximately 20 (26 dB) in the passband.

The step response (Figure 2.17) shows a typical second-order filter behavior, with an adequate rise time and no significant overshoot.

The comparison between simulation and measurements in the Bode diagram (Figure 2.18) shows good agreement, confirming that the design meets the frequency and gain specifications.

Small deviations in the component values do not significantly affect the system performance, and the anti-aliasing filter fulfills its function of attenuating frequencies above 40 kHz, protecting the ADC from possible aliasing.

Additionally, it is observed that the total noise at the driver output is approximately  $40,7 \mu V$  RMS, which contributes to the limitation of the total system SNR.

Obtaining a total SNR of 83.95 dB, the system is capable of achieving an effective resolution of approximately 13.65 bits, which is suitable for many data acquisition applications, although it does not fully exploit the theoretical 16-bit capability of the ADC.

In conclusion, if we wanted to use the full resolution of the ADC, it would be necessary to reduce the driver noise or increase the amplitude of the input signal in order to better utilize the ADC dynamic range.

## 2.3 Switched Capacitor Filter

### 2.3.1 Task Description

A 5th-order clock-tunable switched capacitor filter based on the LTC1063 (dual  $\pm 5V$  supply) was implemented. A non-inverting preamplifier stage using the LM4562 with a gain of 100 was placed in front of the filter.

The frequency response was measured for two clock frequencies (1 MHz and 500 kHz) and compared in a Bode plot. The filter behavior near the clock frequency was investigated in the time domain, including possible clock feedthrough effects.

The total output noise was measured using additional amplification stages, and the input-referred noise voltage was determined for different source resistances. Finally, the SNR and ENOB were calculated for a full-scale sine wave.

### 2.3.2 Schematic

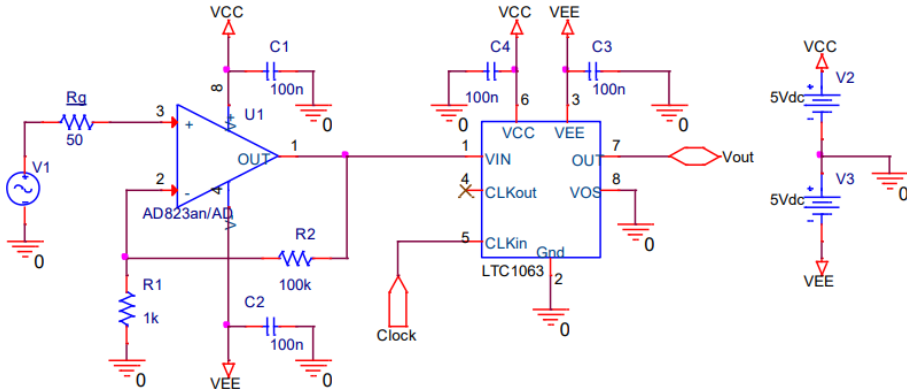


Figure 2.19: Schematic of the switched-capacitor filter with pre-amplifier stage.

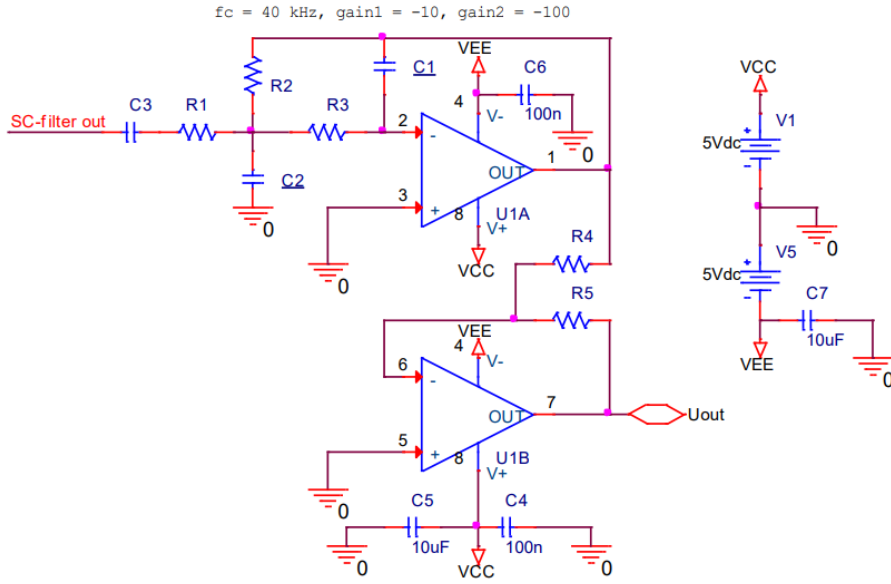


Figure 2.20: Schematic of the low pass filter and amplifier for noise measurement.

### 2.3.3 Formulas and Calculations

#### Thermal Noise of the Source Resistance

The thermal noise density generated by a resistor is given by:

$$e_{n,density} = \sqrt{4kTR_s} \quad (2.27)$$

where:

- $k = 1.38 \times 10^{-23} J/K$  (Boltzmann constant)
- $T = 300 K$  (room temperature)
- $R_s$  is the source resistance

The total RMS noise voltage over a given bandwidth  $B$  is:

$$V_{noise} = \sqrt{4kTB R_s} \quad (2.28)$$

#### Cut-off Frequency of the MAX295

The switched-capacitor filter used in this experiment is the MAX295, which has a clock-to-cutoff frequency ratio of 50:1.

$$f_c = \frac{f_{CLK}}{50} \quad (2.29)$$

For a clock frequency of 1 MHz:

$$f_c = \frac{1,000,000}{50} = 20,000 \text{ Hz} = 20 \text{ kHz} \quad (2.30)$$

For a clock frequency of 500 kHz:

$$f_c = \frac{500,000}{50} = 10,000 \text{ Hz} = 10 \text{ kHz} \quad (2.31)$$

### Noise Bandwidth Correction

Since the filter is an 8th-order Butterworth filter, the noise bandwidth is not equal to the cut-off frequency. A correction factor must be applied. This correction factor can be found in [4] For an 8th-order Butterworth filter:

$$B_{noise} = 1.006455 \cdot f_c \quad (2.32)$$

For  $f_c = 20 \text{ kHz}$ :

$$B_{noise} = 1.006455 \cdot 20000 = 20129.1 \text{ Hz} \quad (2.33)$$

$$\sqrt{B_{noise}} = 141.877 \quad (2.34)$$

### Total System Gain

The complete system gain is:

$$A_{total} = 100 \cdot 1 \cdot 10 \cdot 100 = 100000 \quad (2.35)$$

### Input-Referred Noise

The input-referred noise is calculated as:

$$U_{noise,in} = \frac{U_{noise,out}}{A_{total}} \quad (2.36)$$

## Noise Spectral Density

$$e_n = \frac{U_{noise,in}}{\sqrt{B_{noise}}} \quad (2.37)$$

## Measured Results

Input signal (sine wave):

$$V_{signal,RMS} = \frac{50 \text{ mV}_{pp}}{2 \cdot \sqrt{2}} = 17.67 \text{ mV}_{RMS} \quad (2.38)$$

### Case 1: Input connected to GND

$$U_{noise,out} = 99.69 \text{ mV} \quad (2.39)$$

$$U_{noise,in} = \frac{99.69 \text{ mV}}{100000} = 0.9969 \mu\text{V} \quad (2.40)$$

$$e_n = \frac{0.9969 \times 10^{-6}}{141.877} = 7.03 \text{ nV}/\sqrt{\text{Hz}} \quad (2.41)$$

Since we need an input signal to calculate the SNR, we assume that the input signal is 50 mVpp.

$$SNR = 20 \log_{10} \left( \frac{17.67 \text{ mV}}{0.9969 \mu\text{V}} \right) = 84.97 \text{ dB} \quad (2.42)$$

$$ENOB = \frac{SNR - 1.76}{6.02} = 13.82 \text{ bits} \quad (2.43)$$

### Case 2: $R_s = 51 \Omega$

$$U_{noise,out} = 101.24 \text{ mV} \quad (2.44)$$

$$U_{noise,in} = \frac{101.24 \text{ mV}}{100000} = 1.0124 \mu\text{V} \quad (2.45)$$

$$e_n = \frac{1.0124 \times 10^{-6}}{141.877} = 7.13 \text{ nV}/\sqrt{\text{Hz}} \quad (2.46)$$

SNR and ENOB were calculated assuming an input sine wave of 50 mVpp (17.67 mV RMS)

$$SNR = 20 \log_{10} \left( \frac{17.67 \text{ mV}}{1.0124 \mu V} \right) = 84.83 \text{ dB} \quad (2.47)$$

$$ENOB = \frac{84.83 - 1.76}{6.02} = 13.80 \text{ bits} \quad (2.48)$$

**Case 3:**  $R_s = 100 \text{ k}\Omega$

$$U_{noise,out} = 122.2 \text{ mV} \quad (2.49)$$

$$U_{noise,in} = \frac{122.2 \text{ mV}}{100000} = 1.222 \mu V \quad (2.50)$$

$$e_n = \frac{1.222 \times 10^{-6}}{141.877} = 8.61 \text{ nV}/\sqrt{\text{Hz}} \quad (2.51)$$

SNR and ENOB were calculated assuming an input sine wave of 50 mVpp (17.67 mV RMS)

$$SNR = 20 \log_{10} \left( \frac{17.67 \text{ mV}}{1.222 \mu V} \right) = 83.18 \text{ dB} \quad (2.52)$$

$$ENOB = \frac{83.18 - 1.76}{6.02} = 13.54 \text{ bits} \quad (2.53)$$

### 2.3.4 Table(s) with Measurement Results

Table 2.6: Component values for switched capacitor filter

	Calculated	Chosen	Measured
$R_g$ in $\Omega$	50	50	51.085
$R_{g2}$ in $\text{k}\Omega$	100	100	99.959
$R_1$ in $\Omega$	-	1000	994.81
$R_2$ in $\text{k}\Omega$	-	100	99.761
$C_1$ in $\text{nF}$	-	100	-
$C_2$ in $\text{nF}$	-	100	-
$C_3$ in $\text{nF}$	-	100	-
$C_4$ in $\text{nF}$	-	100	-

Table 2.7: Component values for low pass filter and noise measurement amplifier

	Calculated	Chosen	Measured
$R_1$ in $\Omega$	-	820	817
$R_2$ in $k\Omega$	-	8.2	8.1602
$R_3$ in $k\Omega$	-	2.7	2.6888
$R_4$ in $\Omega$	1000	1000	996.6
$R_5$ in $k\Omega$	100	100	99.585
$C_1$ in $pF$	-	150	155
$C_2$ in $nF$	-	4.7	4.61
$C_3$ in $\mu F$	-	1.5	1.56
$C_4$ in $nF$	-	100	-
$C_5$ in $\mu F$	-	10	-
$C_6$ in $nF$	-	100	-
$C_7$ in $\mu F$	-	10	-

The measured resistor values confirm the 1% tolerance specification. Since the switched capacitor filter cutoff frequency is defined by the clock frequency rather than absolute capacitor values, the passive component tolerances have only minor influence on the filter characteristics.

The measurements for the bode plot can be found at the appendix in table A.3 and A.4.

When reducing the clock frequency from 1 MHz to 500 kHz, the cutoff frequency of the switched capacitor filter decreases proportionally. This confirms the theoretical relationship:

$$f_c \propto f_{CLK}$$

The measured data shows approximately half the cutoff frequency compared to the 1 MHz case, which validates the internal switched capacitor principle. Phase wrapping at  $\pm 180^\circ$  is again visible due to measurement representation.

Table 2.8: Noise and Performance Summary

Adjusted $U_{in(pp)}$	$f$ (MHz)	$R_g$ ( $\Omega$ )	$U_{out,noise(rms)}$ (mV)	SNR (dB)	ENOB (bits)	$U_{in,noise(rms)}$ ( $\mu V$ )	$e_n$ (nV/ $\sqrt{Hz}$ )
50	1	GND	99.69	84.97	13.82	0.997	7.03
50	1	51	101.24	84.83	13.80	1.012	7.13
50	1	100000	122.20	83.18	13.54	1.222	8.61

### 2.3.5 Curves & Diagrams

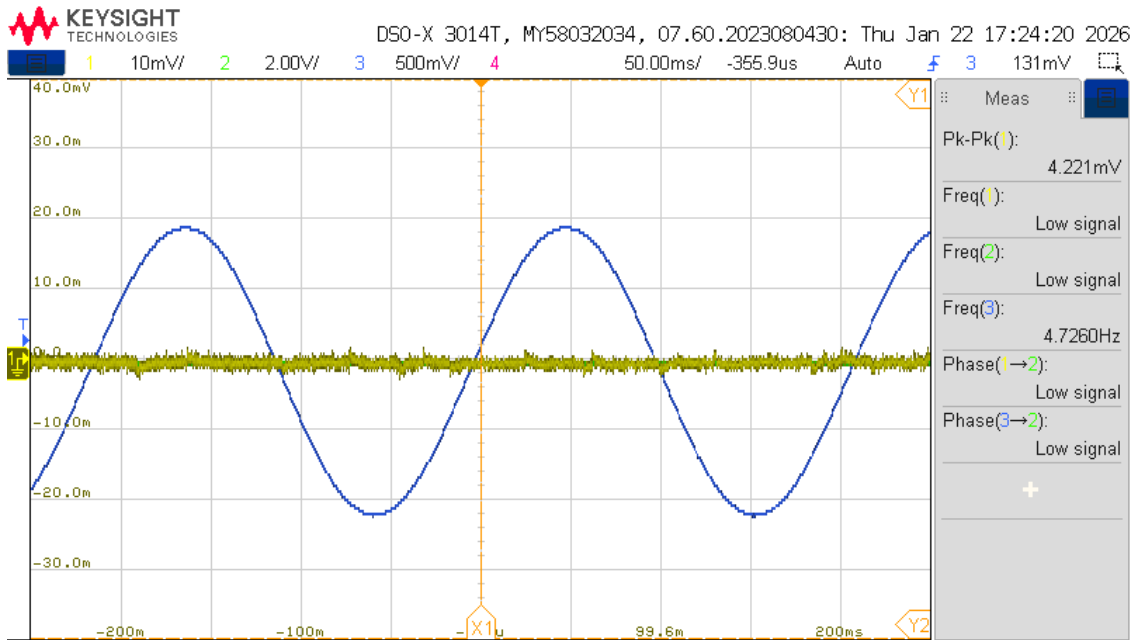


Figure 2.21: Output (blue) of the switched capacitor filter with the input frequency near the tuning frequency.

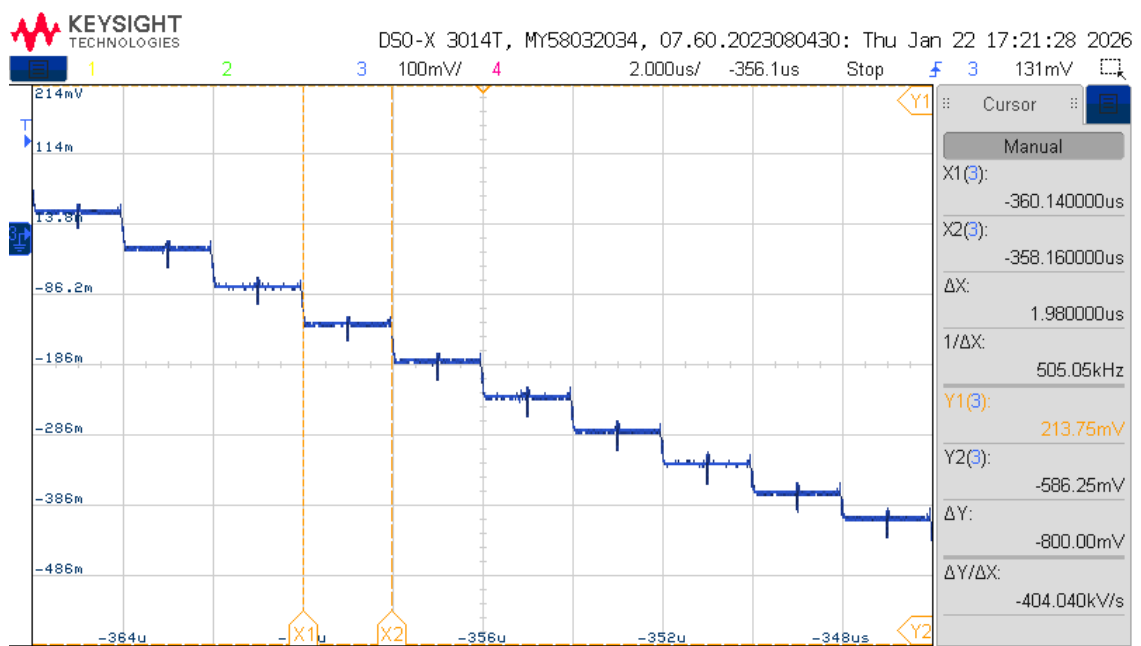


Figure 2.22: Close up of the switched-capacitor filters output signal. Each step is one switching operation of the capacitors.

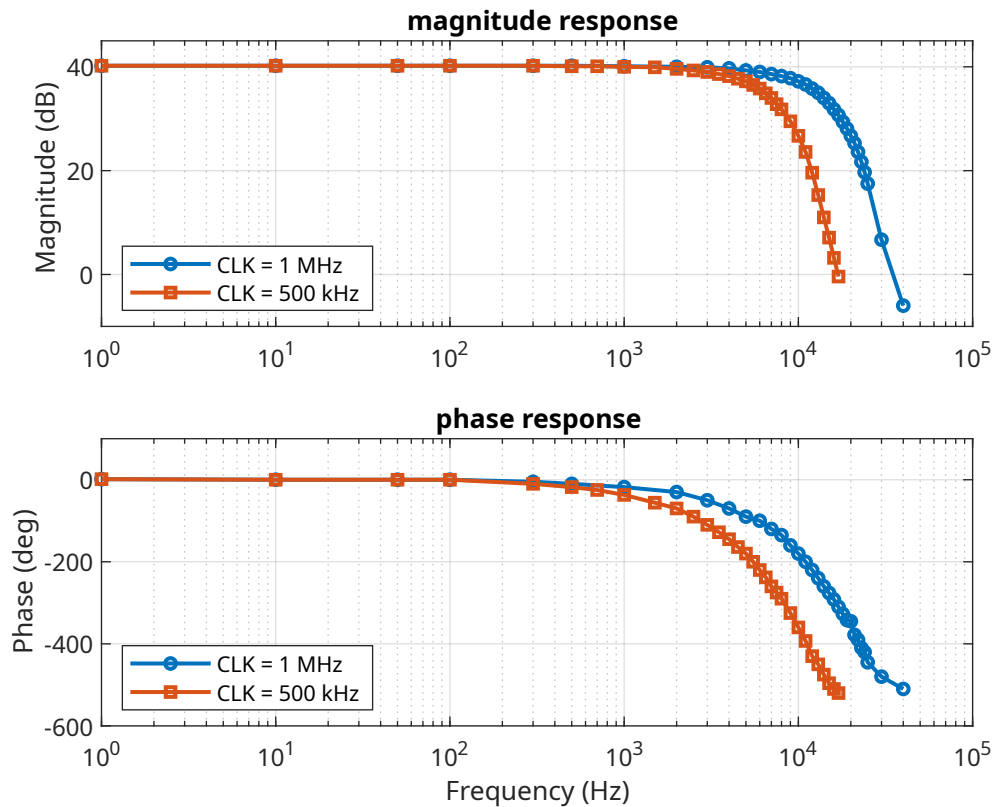


Figure 2.23: Bode plot displaying measured phase and magnitude responses of the switched capacitor filter, one with a tuning frequency of 1 MHz, one with a tuning frequency of 500 kHz.

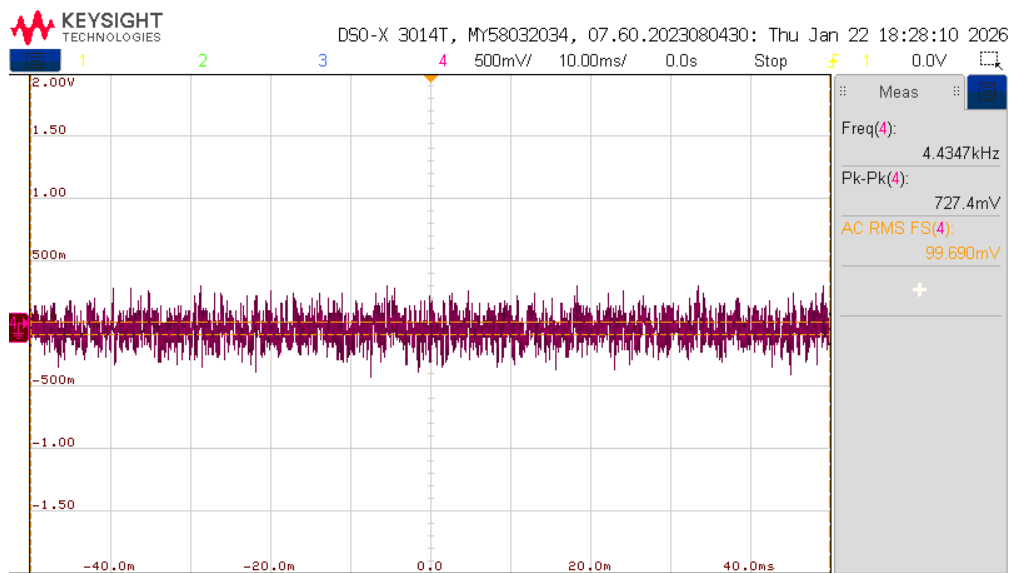


Figure 2.24: Measurement of the total output noise voltage with the input shorted to ground and the SC-filter tuning frequency set to 1 MHz.

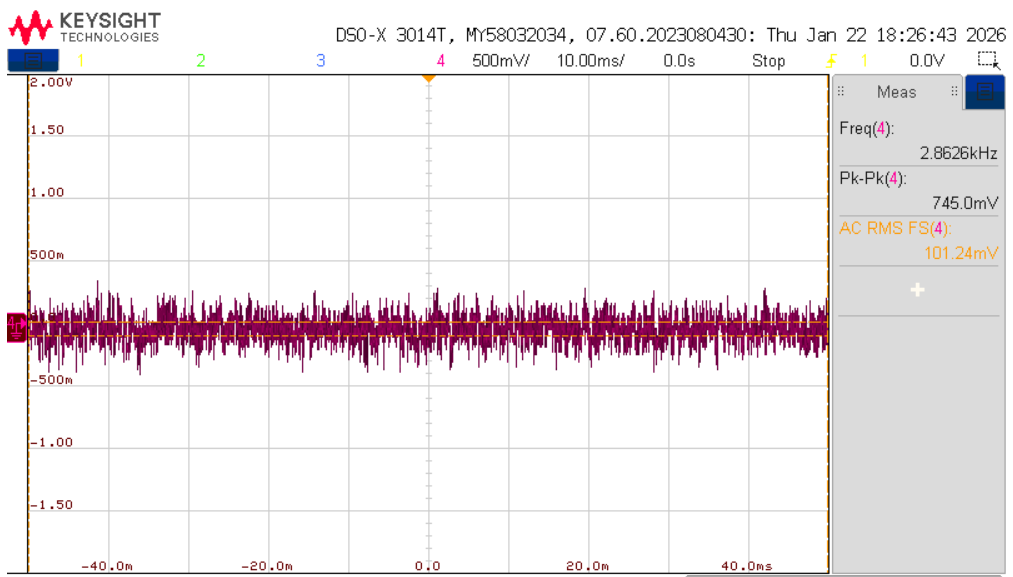


Figure 2.25: Measurement of the total output noise voltage with the input  $51\ \Omega$  and the SC-filter tuning frequency set to 1 MHz.

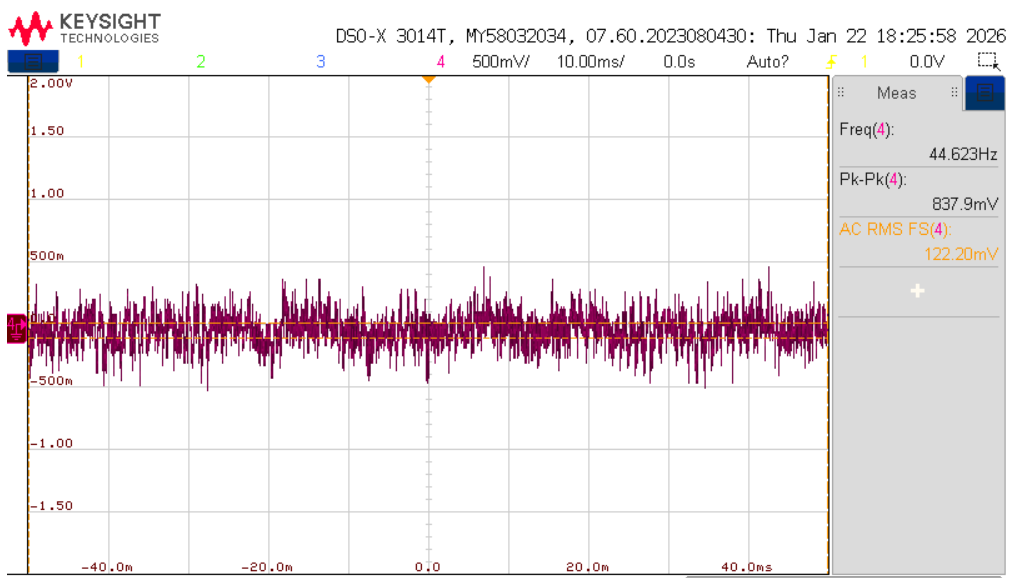


Figure 2.26: Measurement of the total output noise voltage with the input shorted  $100k\ \Omega$  and the SC-filter tuning frequency set to 1 MHz.

### 2.3.6 Discussion of Measurement Results

In principle, for our measurements we had to use the LT1063 switched capacitor filter, but since we did not have it in our component stock, we used the MAX295, which is an 8th order switched capacitor filter. As we can see in Figure 2.23, the MAX295 switched capacitor filter has a magnitude response that shows an active low pass. The gain in the passband is approximately 40 dB, which

indicates that the filter amplifies signals within its passband frequency range. The cutoff frequency is around 20 kHz for a tuning frequency of 1 MHz, and around 10 kHz for a tuning frequency of 500 kHz. This confirms the theoretical relationship between the cutoff frequency and the tuning frequency in switched capacitor filters. [2]

When the filter input frequency is close to the tuning frequency, a ‘low signal’ is observed in the oscilloscope measurement section, as shown in Figure 2.21. This is because the input frequency is much higher than the filter cutoff frequency, resulting in significant signal attenuation. Figure 2.22 shows a close-up of the output signal from the switched capacitor filter, where each step represents a capacitor switching operation. This is characteristic of switched capacitor filters, where the signal is sampled and processed based on the switching frequency.

Subsequently, the total output noise voltage was measured by connecting the output of the switched capacitor filter to an amplifier circuit to measure the noise. Figure 2.24 shows the measurement of the total output noise voltage with the input connected to ground. Figure 2.25 shows the measurement of the total output noise voltage with the  $51\ \Omega$  input. Figure 2.26 shows the measurement of the total output noise voltage with the input at  $100k\ \Omega$ . Table 2.8 summarises the results of the noise and performance measurements for different input resistances.

By observing these values, we can determine that when the input signal is connected to ground, we are measuring the noise voltage at the output of the entire set of amplifier stages. Then, as the input resistance increases, the total output noise voltage also increases. This is because the thermal noise generated by the input resistance increases with its value, resulting in higher noise voltage at the output of the switched capacitor filter.

This leads us to the conclusion that at low resistances, op-amp noise dominates, while at high resistances, thermal noise from the input resistance dominates.

## Bibliography

- [1] P. Horowitz and W. Hill, *The Art of Electronics*, 3rd ed., Cambridge University Press, 2015.
- [2] Maxim Integrated, *MAX295 8th-Order Low-Pass Switched-Capacitor Filter Datasheet*.
- [3] A. S. Sedra and K. C. Smith, *Microelectronic Circuits*, Oxford University Press.
- [4] S. Winder, *Analog and Digital Filter Design*, 2nd ed., Elsevier, 2002. [Online]. Available: [https://www.freestompboxes.org/members/archive/WINDER,%20S.%20\(2002\).%20Analog%20and%20Digital%20Filter%20Design%20\(2nd%20ed.\).pdf](https://www.freestompboxes.org/members/archive/WINDER,%20S.%20(2002).%20Analog%20and%20Digital%20Filter%20Design%20(2nd%20ed.).pdf)

# Equipment

- Benchtop Multimeter

Manufacturer: Agilent

Model: 34450A

- Oscilloscope

Manufacturer: Keysight

Model: DSO-X 3014T

- Function Generator

Manufacturer: Keysight

Model: 33500B

- LCR-Meter

Manufacturer: Keysight

Model: U1733C



---

Graz, February 21, 2026

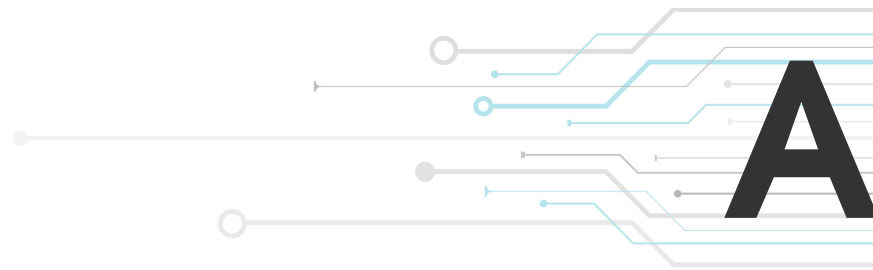
Lorenz Buchinger



---

Agustín Sevil de Llobet





# Appendix

## A.1 Calculations

### A.1.1 Active Band-pass Filter

ACD - Lektur 1

$$\text{I}_2 = \frac{U_{\text{out}}}{R_2} \quad \text{I}_{C1} = -U_{\text{out}} + U_{C2}$$

$$U_{C2} = \frac{U_{\text{out}}}{S C_2 R_2}$$

$$I_{C1} = \frac{U_{C1}}{C_1} = -S(C_1 U_{\text{out}} + \frac{U_{\text{out}}}{S C_2 R_2})$$

$$\text{II} \quad U_{C2} + U_{R_3} = 0 \rightarrow U_{R_3} = -U_{C2}$$

$$\text{III} \quad U_{R_1} + U_{R_3} - U_{\text{in}} = 0 \rightarrow U_{R_1} = U_{\text{in}} - U_{R_3}$$

$$I_3 = -\frac{U_{C2}}{R_3} = -\frac{U_{\text{out}}}{S C_2 R_2 R_3} \quad I_1 = \frac{U_{R_1}}{R_1} = \frac{U_{\text{in}}}{R_1} + \frac{U_{\text{out}}}{S C_2 R_2 R_1}$$

$$I_1 + I_2 = I_3 + I_{C1} \rightarrow \frac{U_{\text{in}}}{R_1} + \frac{U_{\text{out}}}{S C_2 R_2 R_1} + \frac{U_{\text{out}}}{R_2} = -\frac{U_{\text{out}}}{S C_2 R_2 R_3} - U_{\text{out}} \cdot S C_1 + \frac{U_{\text{out}} \cdot C_1}{C_2 R_2}$$

$$\rightarrow \frac{U_{\text{in}}}{R_1} = -U_{\text{out}} \left( \frac{1}{R_2} + \frac{C_1}{C_2 R_2} + S C_1 C_2 + \frac{1}{S C_2 R_1 R_2} + \frac{1}{S C_2 R_2 R_3} \right)$$

$$\rightarrow S \frac{U_{\text{in}}}{R_1} = -U_{\text{out}} \cdot \left( S \frac{C_1 + C_2}{C_2 R_2} + S^2 C_1 + \frac{R_1 + R_3}{C_2 R_1 R_2 R_3} \right) \rightarrow \frac{U_{\text{out}}}{U_{\text{in}}} = -\frac{\frac{1}{R_1}}{\frac{R_1 + R_3}{C_2 R_1 R_2 R_3} + S \frac{C_1 + C_2}{C_2 \cdot R_2} + S^2 C_1}$$

$$\rightarrow H(s) = -\frac{\frac{R_2 \cdot R_3}{R_1 + R_3} \cdot S C_2}{1 + S \frac{R_1 R_3 (C_1 + C_2)}{R_1 + R_3} + S^2 \frac{R_1 R_2 R_3 C_1 C_2}{R_1 R_3}}$$

Lernplan teileband Pass  $\rightarrow$  2.5.4 Röhrschaltung Anwendung:  $P \Rightarrow \frac{1}{\Delta \Omega} (P + \frac{1}{P})$  with  $\frac{1}{\Delta \Omega} = Q \Rightarrow S \Rightarrow \frac{S^2 + \omega_0^2}{BS}$

$$H_{LP}(s) = \frac{1}{S^2 + \alpha s + \omega_0^2} \xrightarrow{\text{substitution}} H_{BP}(s) = \frac{1}{(\frac{S^2 + \omega_0^2}{BS})^2 + \alpha \left( \frac{S^2 + \omega_0^2}{BS} \right) + \omega_0^2} \rightarrow B^2 S^2 \rightarrow \omega_0 = 2\pi f_0$$

$$B = \frac{\omega_0}{Q}$$

$$\rightarrow H_{BP}(s) = \frac{B^2 S^2}{(S^2 + \omega_0^2)^2 + \alpha BS(S^2 + \omega_0^2) + \omega_0^2 B^2 S^2} \rightarrow \left. \begin{array}{l} (S^2 + \omega_0^2)^2 = S^4 + 2\omega_0^2 S^2 + \omega_0^4 \\ \alpha BS(S^2 + \omega_0^2) = \alpha B S^3 + \alpha B \omega_0^2 S \\ B^2 S^2 \end{array} \right\} \rightarrow \text{Polarisieren}$$

$$\rightarrow D(s) = S^4 + \alpha B S^3 + (2\omega_0^2 + \omega_0^2 B^2) S^2 + \alpha B \omega_0^2 S + \omega_0^4 \rightarrow \text{Substitute } B \rightarrow$$

$$\rightarrow D_{std}(s) = S^4 + \frac{\omega_0}{Q} S^3 + \left( 2\omega_0^2 + \frac{\omega_0^2}{Q^2} \right) S^2 + \frac{\omega_0^3}{Q} S + \omega_0^4$$

computation coefficients

$$\left[ \begin{array}{c} 1 \\ 2\omega_0^2 \\ \omega_0^2 \\ \omega_0^3 \end{array} \right]$$

$$\left[ \begin{array}{c} 1 \\ 2\omega_0^2 \\ \omega_0^2 \\ \omega_0^3 \end{array} \right]$$

Contract Park &

$$D_0(s) = s^4 + \frac{\omega_{0i}}{Q} s^3 + \left(2\omega_{0i}^2 + \frac{\omega_{0i}^2}{Q^2}\right) s^2 + \frac{\omega_{0i}^3}{Q} s + \omega_{0i}^4 \rightarrow \omega_{01} = \alpha \omega_0, \omega_{02} = \frac{\omega_0}{\alpha}$$

$$D_1(s) = s^4 + \frac{\alpha \omega_0}{Q} s^3 + \left(2\alpha^2 \omega_0^2 + \frac{\alpha^2 \omega_0^2}{Q^2}\right) s^2 + \frac{\alpha^3 \omega_0^3}{Q} s + \alpha^4 \omega_0^4$$

$$D_2(s) = s^4 + \frac{\omega_0}{\alpha Q} s^3 + \left(\frac{2\omega_0^2}{\alpha^2} + \frac{\omega_0^2}{\alpha^2 Q^2}\right) s^2 + \frac{\omega_0^3}{\alpha^3 Q} s + \frac{\omega_0^4}{\alpha^4} \quad \left. \begin{array}{l} D_3(s) = D_1(s) \cdot D_2(s) \\ \end{array} \right\} \rightarrow$$

$$\rightarrow D_3(s) (s^4 + A_3 s^3 + A_2 s^2 + A_1 s + A_0) (s^4 + B_3 s^3 + B_2 s^2 + B_1 s + B_0)$$

Gerade Frequenz

$$\underline{f_L = 4000 \text{ Hz} \quad f_U = 5000 \text{ Hz} \rightarrow f_0 = \sqrt{f_L f_U} = 4472,14 \text{ Hz} \quad \omega_0 = 2\pi \cdot f_0 = 2\pi \cdot 4472,14 = 281098,3}$$

$$BW = f_U - f_L = 1000 \text{ Hz} \quad Q = \frac{f_0}{BW} = 4,42 \quad \Delta \omega_m = \frac{BW}{f_0} = 0,2236 \quad \text{All } C = 10 \mu\text{F}$$

parallel Resonator

Substitution

$$P = \frac{1}{\Delta \Omega} \left( P + \frac{1}{P} \right) \text{ with } \frac{1}{\Delta \Omega} = Q \rightarrow H(s) = \frac{H_0}{1 + a_1 \left( \frac{1}{\Delta \Omega} \left( P + \frac{1}{P} \right) \right) + b_1 \left( \frac{1}{\Delta \Omega} \left( P + \frac{1}{P} \right) \right)^2} \rightarrow$$

$$\rightarrow \frac{H_0}{1 + \frac{a_1 P}{\Delta \Omega} + \frac{a_1}{\Delta \Omega P} + \frac{b_1 P^2}{\Delta \Omega^2} + \frac{2b_1}{\Delta \Omega^2} + \frac{b_1}{\Delta \Omega^2 P^2}} \rightarrow \frac{\frac{\Delta \Omega^2 P^2}{1}}{1} \rightarrow$$

$$\rightarrow \frac{H_0 \Delta \Omega^2 P^2}{\Delta \Omega^2 P^2 + \frac{a_1 \Delta \Omega^2 P^3}{\Delta \Omega} + \frac{a_1 \Delta \Omega^2 P^2}{\Delta \Omega P} + \frac{b_1 P^4 \Delta \Omega^2}{\Delta \Omega^2} + \frac{2b_1 \Delta \Omega^2 P^2}{\Delta \Omega^2} + \frac{b_1 \Delta \Omega^2 P^2}{\Delta \Omega^2 P^2}} \rightarrow$$

$$\rightarrow \frac{H_0 \Delta \Omega^2 P^2}{\Delta \Omega^2 P^2 + a_1 \Delta \Omega^2 P^3 + a_1 \Delta \Omega^2 P^2 + b_1 P^4 + 2b_1 P^2 + b_1} \rightarrow \frac{1}{b_1} \rightarrow \frac{\frac{H_0 \Delta \Omega^2 P^2}{b_1}}{\frac{\Delta \Omega^2 P^2}{b_1} + \frac{a_1 \Delta \Omega^2 P^3}{b_1} + \frac{a_1 \Delta \Omega^2 P^2}{b_1} + \frac{b_1 P^4 + 2b_1 P^2 + b_1}{b_1}}$$

Normalization  $\rightarrow = \frac{\frac{H_0 \Delta \Omega^2 P^2}{b_1}}{1 + \frac{a_1}{b_1} \Delta \Omega P + \left[ 2 + \frac{\Delta \Omega^2}{b_1} \right] P^2 + \frac{a_1}{b_1} \Delta \Omega P^3 + P^4}$

Script: 1<sup>st</sup> order Lengyel:

$$H(P) = \frac{\frac{H_0}{b_1} \Delta \Omega^2 P^2}{\left[ 1 + \frac{a_1}{Q_i} P + (\alpha P)^2 \right] \left[ 1 + \frac{1}{Q_i} \left( \frac{P}{\alpha} \right) + \left( \frac{P}{\alpha} \right)^2 \right]}$$

denominator:

$$\left[ 1 + \frac{1}{Q_i} \left( \frac{P}{\alpha} \right) + \left( \frac{P}{\alpha} \right)^2 \right] + \left[ \frac{\alpha}{Q_i} P + \frac{\alpha P^2}{Q_i^2 \alpha} + \frac{P^3}{\alpha Q_i} \right] + \left[ (\alpha P)^2 + \frac{\alpha P^3}{Q_i} + P^4 \right] \rightarrow P \text{ common denominator} \rightarrow$$

$$\infty = 1 + P \left[ \frac{1}{Q_i \alpha} + \frac{\alpha}{Q_i} \right] + P^2 \left[ \frac{1}{\alpha^2} + \frac{1}{Q_i^2} + \alpha^2 \right] + P^3 \left[ \frac{1}{\alpha Q_i} + \frac{\alpha}{Q_i} \right] + P^4$$

2

Escaneado con CamScanner

Figure A.2: Page 2 of the hand written calculations for the active band-pass filter.

Mitglieder zu bestimmen:

$$1 + P \left[ \frac{a_1}{b_1} \Delta \Omega \right] + P^2 \left[ 2 + \frac{\Delta \Omega^2}{b_1} \right] + P^3 \left[ \frac{a_1}{b_1} \Delta \Omega \right] + P^4$$

$$P^1: \frac{1}{Q_i \alpha} + \frac{\alpha}{Q_i} = \frac{a_1}{b_1} \Delta \Omega \rightarrow \frac{1 + \alpha^2}{Q_i \alpha} = \frac{a_1 \Delta \Omega}{b_1} \rightarrow \frac{1}{(1 + \alpha^2)} = \frac{a_1}{b_1 + b_1 \alpha^2} \text{ mit } \Delta \Omega \rightarrow$$

$$\rightarrow \cancel{(1 + \alpha^2)^{-1}} \rightarrow Q_i \alpha = \frac{b_1 + b_1 \alpha^2}{a_1 \Delta \Omega} \rightarrow \frac{1}{\alpha} \rightarrow Q_i = \frac{b_1 + b_1 \alpha^2}{a_1 \Delta \Omega \alpha} \quad \text{I}$$

$$P^2: \frac{1}{\alpha^2} + \frac{1}{Q_i^2} + \alpha^2 = 2 + \frac{\Delta \Omega^2}{b_1} \rightarrow \text{Substitution QI} \rightarrow \frac{1}{\alpha^2} + \frac{1}{\frac{(b_1 + b_1 \alpha^2)^2}{a_1 \Delta \Omega \alpha}} + \alpha^2 = 2 + \frac{\Delta \Omega^2}{b_1}$$

$$\text{Battermann} \quad \left. \begin{array}{l} a_1 = \sqrt{2} \\ b_1 = 1 \end{array} \right\} \text{Tabellen} \quad \Delta \Omega = \frac{f_{\max} - f_{\min}}{f_0} = \frac{1000}{1472,1} = 0,2236 \quad f_{m1} = \frac{f_0}{\alpha} = 4131,53 \\ f_0 = \sqrt{f_{\min} f_{\max}} = \sqrt{1000 \cdot 5000} = 1472,1 \text{ Hz} \quad f_{m2} = f_0 \alpha = 41840,82$$

$$\text{Solve eq (I) with Tj-mspire CX II F second} \rightarrow \alpha BW = 1,08244 \rightarrow Q_{BSW} = \frac{b_1 + b_1 \alpha^2}{a_1 \Delta \Omega \alpha} = 634444$$

$$C_1 = C_2 = 10 \text{ nF} \rightarrow C \quad B = \frac{C_1 + C_2}{2 \pi R_2 C_1 C_2} = \frac{2 \times 10}{2 \pi R_2 C^2} = \frac{1}{\pi C R_2} \rightarrow R_2 = \frac{1}{\pi C B} = 488799 \text{ k}\Omega$$

$$H_T = -\frac{C R_2}{2 \pi R_1} = -\frac{R_2}{2 R_1} \rightarrow |H_T| = \frac{R_2}{2 R_1} \Rightarrow R_1 = \frac{R_2}{2 H_T} = 5447,84 \Omega$$

$$H_T = Q_i \Delta \Omega \sqrt{\frac{H_{mid}}{b_1}} = 6344 \cdot 0,2236 \cdot \sqrt{\frac{10}{1}} = 4,48618$$

$$R_3 = \frac{R_1}{(R_1 R_2 \frac{f_{\max}^2}{f_0^2} - 1)(2 \pi C)^2} = 303,59 \Omega$$

$$BW2: \quad R_S = \frac{1}{\pi C B} \rightarrow B = \frac{f_{m2}}{Q} = 763'005 \rightarrow R_S = 41'7179 \text{ k}\Omega \quad R_4 = \frac{R_S}{2 H_T} = 4649,61 \Omega$$

$$R_6 = \frac{R_4}{(R_4 R_S \frac{f_{\max}^2}{f_0^2} - 1)(2 \pi C)^2} = 259,107 \Omega$$

Calculated  $\frac{R_1}{R_4} = 5447,84 \Omega$

$R_1 = 5447,84 \Omega$   $R_1 = 5447,84 \Omega$

$R_2 = 488799 \Omega$   $R_2 = 488799 \Omega$

$R_3 = 303,59 \Omega$   $R_3 = 303,59 \Omega$

$B_4 = 4649,61 \Omega$   $R_4 = 4649,61 \Omega$

$R_S = 41'7179 \Omega$   $R_S = 41'7179 \Omega$

$R_6 = 259,107 \Omega$   $R_6 = 259,107 \Omega$

Figure A.3: Page 3 of the hand written calculations for the active band-pass filter.

Chabry 1 Table 12-39, Taitze  $\Rightarrow \left\{ \begin{array}{l} a_1 = 1,0650 \\ b_1 = 1,9305 \end{array} \right\}$ , solve eq I with  $T1-m$  spine CX II- $\Gamma$   $\Rightarrow Q_i = \frac{\omega_i}{\omega_c} = 1,09712$

$$Q_{m1} = \frac{\omega_0}{\omega_{CH}} = 0,9151,94$$

$$\omega_0 = 4472,13 \quad \Delta\omega = 0,2236 \quad Q_{iCH} = 16,2578$$

$$Q_{m2} = \omega_0 \cdot \omega_{CH} = 4,817,03$$

$$H_F = 16,25 \cdot 0,2236 \cdot \sqrt{\frac{\omega_0}{\omega_1}} = 8,27395 \Rightarrow R_2 = \frac{1}{\pi \cdot B \cdot C} \rightarrow B = \frac{Q_{m1}}{Q_i} = 255,381 \Rightarrow R_2 = 124,641 \text{ k}\Omega$$

$$R_1 = \frac{R_2}{2H_F} = 7,53215 \text{ k}\Omega = R_1$$

$$R_3 = \frac{R_4}{(R_1 R_2 Q_{m1}^2 - 1)(2\pi \cdot C)^2} = 117,89 \Omega$$

$$R_S = \frac{1}{\pi B \cdot C} \rightarrow B = \frac{Q_{m2}}{Q_i} = 296,29 \Rightarrow R_S = 107,432 \text{ k}\Omega$$

$$R_4 = \frac{R_S}{2H_F} = \frac{107,432}{2 \cdot 8,27395} = 6,49219 \text{ k}\Omega = R_4$$

$$R_6 = \frac{R_4}{(R_4 R_S Q_{m2}^2 - 1)(2\pi \cdot C)^2} = 101,613 \Omega$$

calculated      €24

$R_1 = 7,53215 \text{ k}\Omega$	$R_1 = 7,5 \text{ k}\Omega$
$R_2 = 124,641 \text{ k}\Omega$	$R_2 = 120 \text{ k}\Omega$
$R_3 = 117,89 \Omega$	$R_3 = 120 \text{ k}\Omega$
$R_4 = 6,49219 \text{ k}\Omega$	$R_4 = 6,2 \text{ k}\Omega$
$R_S = 107,432 \text{ k}\Omega$	$R_S = 110 \text{ k}\Omega$
$R_6 = 101,613 \Omega$	$R_6 = 100 \Omega$

Escaneado con CamScanner

Figure A.4: Page 4 of the hand written calculations for the active band-pass filter.

## A.2 Matlab

## A.3 Measurements

Table A.1: Measured frequency response of the active band-pass filter

Frequency / Hz	Gain / dB	Phase / Degree	Remark
1	-47	-	
10	-45	-	
100	-45	-	
1000	-32	-	
1100	-30	170	
1200	-29.4	165	
1300	-27.9	165	
1400	-25.8	162	

Table A.1: Measured frequency response of the active band-pass filter (continuation)

Frequency / Hz	Gain / dB	Phase / Degree	Remark
1500	-24.3	160	
2000	-17.6	164	
2600	-10	164	
3000	-4.3	158	
3300	0.2	152	
3400	1.9	148	
3500	3.6	145	
3600	5.5	142	
3700	7.4	136	
3800	9.5	130	
3900	11.7	123	
4000	14.2	112	
4100	16.5	100	
4200	18.7	82	<b>-3 dB region</b>
4230	19.3	76	<b>-3 dB region</b>
4300	20.5	62	<b>-3 dB region</b>
4400	21.6	39	
4472.13	22.1	22	Theoretical $f_c$
4500	22.2	16	
4570	22.3	0	Measured $f_c$
4600	22.3	-6	
4700	22	-28	
4800	21.2	-50	
4900	19.9	-70	<b>-3 dB region</b>
4940	19.3	-76	<b>-3 dB region</b>
5000	18.2	-86	<b>-3 dB region</b>
5100	16.4	-100	
5200	14.5	-110	

Table A.1: Measured frequency response of the active band-pass filter (continuation)

Frequency / Hz	Gain / dB	Phase / Degree	Remark
5300	12.7	-119	
5400	11	-126	
5500	9.4	-131	
5600	8	-136	
5700	6.7	-139	
5800	5.5	-142	
5900	4.3	-145	
6000	3.2	-147	
6100	2.2	-150	
6200	1.2	-152	
6300	0.3	-154	
6400	-0.5	-156	
6700	-2.8	-160	
7500	-7.5	-171	
8000	-9.7	-	
9000	-13.3	-	
10000	-16.4	-	
50000	-32.5	-	

Table A.2: Measured frequency response of the ADC-driver and anti-aliasing filter

Frequency / Hz	Gain / dB	Phase / Degree
3	-6.80	80
7	0.40	85
10	3.40	87
20	9.30	80
40	15.00	73
50	16.80	69

Table A.2: Measured frequency response of the ADC-driver and anti-aliasing filter (continuation)

Frequency / Hz	Gain / dB	Phase / Degree
60	18.10	66
70	19.20	61
80	20.10	59
90	20.90	56
100	21.50	54
110	22.00	51
120	22.40	48
130	22.80	46
135	23.00	45
140	23.10	44
150	23.40	42
160	23.70	40
170	23.90	38
180	24.10	36
190	24.20	35
200	24.40	34
210	24.50	33
220	24.60	31
230	24.70	30
240	24.80	29
260	25.00	27
280	25.10	25
300	25.20	24
330	25.40	22
350	25.40	20
400	25.60	18
450	25.70	16
500	25.80	14

Table A.2: Measured frequency response of the ADC-driver and anti-aliasing filter (continuation)

Frequency / Hz	Gain / dB	Phase / Degree
600	25.80	10
750	25.90	8
825	25.90	7
1000	26.00	6
1250	26.00	4
1500	26.00	2
1750	26.00	0
2250	26.00	-1
2500	26.00	-2
2750	26.00	-3
3000	26.00	-4
3500	26.00	-5
6000	26.00	-11
10000	25.90	-18
11000	25.90	-21
12000	25.90	-23
13000	25.80	-28
14000	25.80	-30
15000	25.80	-31
16000	25.70	-34
17000	25.70	-35
18000	25.60	-37
19000	25.60	-40
20000	25.50	-42
22000	25.40	-48
24000	25.20	-54
26000	25.00	-56
28000	24.70	-60

Table A.2: Measured frequency response of the ADC-driver and anti-aliasing filter (continuation)

Frequency / Hz	Gain / dB	Phase / Degree
30000	24.40	-66
32000	24.10	-72
33000	24.00	-75
34000	23.80	-75
35000	23.60	-78
37000	23.20	-80
38000	23.00	-83
39000	22.80	-84
40000	22.60	-86
45000	21.50	-93
50000	20.40	-106
55000	19.20	-109
60000	18.00	-114
65000	16.90	-120
70000	15.50	-122
75000	14.50	-125
100000	9.90	-130
120000	6.80	-140
150000	3.30	-156
190000	0.00	-180
200000	-1.00	-180

Table A.3: Measured frequency and phase response of switched capacitor filter with a tuning frequency of 500 kHz

Input Frequency / Hz	Gain / dB	Phase / Degree
1	40.2	1.4
10	40.2	0
50	40.2	0

Table A.3: Measured frequency and phase response of switched capacitor filter with a tuning frequency of 500 kHz (continuation)

Input Frequency / Hz	Gain / dB	Phase / Degree
100	40.2	0
300	40.2	-10
500	40.1	-18
700	40.1	-25
1000	40.0	-37
1500	39.9	-56
2000	39.6	-70
2500	39.3	-90
3000	39.0	-110
3500	38.6	-128
4000	38.2	-145
4500	37.7	-164
5000	37.2	180
5500	36.5	160
6000	35.8	140
6500	34.9	122
7000	34.0	100
7500	32.8	85
8000	31.8	70
9000	29.5	35
10000	26.7	0
11000	23.6	-33
12000	19.6	-70
13000	15.3	-90
14000	11.0	-115
15000	7.1	-136
16000	3.2	-150

Table A.3: Measured frequency and phase response of switched capacitor filter with a tuning frequency of 500 kHz (continuation)

<b>Input Frequency / Hz</b>	<b>Gain / dB</b>	<b>Phase / Degree</b>
17000	-0.4	-160

Table A.4: Measured frequency and phase response of switched capacitor filter with a tuning frequency of 1 MHz

<b>Input Frequency / Hz</b>	<b>Gain / dB</b>	<b>Phase / Degree</b>
1	40.2	1.33
10	40.2	0
50	40.2	0
100	40.2	0
300	40.2	-5
500	40.2	-10
1000	40.1	-18
2000	40.0	-30
3000	39.9	-50
4000	39.7	-70
5000	39.3	-90
6000	39.0	-100
7000	38.6	-120
8000	38.2	-135
9000	37.8	-160
10000	37.2	180
11000	36.6	160
12000	35.8	140
13000	35.0	120
14000	34.0	100
15000	33.0	84
16000	31.8	68

Table A.4: Measured frequency and phase response of switched capacitor filter with a tuning frequency of 1 MHz (continuation)

<b>Input Frequency / Hz</b>	<b>Gain / dB</b>	<b>Phase / Degree</b>
17000	30.7	50
18000	29.4	33
19000	28.1	18
20000	26.7	15
21000	25.3	-18
22000	23.6	-30
23000	21.7	-50
24000	19.7	-60
25000	17.5	-85
30000	6.7	-120
40000	-6.0	-150